EUROPEAN ORGANIZATION FOR NUCLEAR RESEARCH (CERN)

CERN-EP/2016-050
2016/10/10

CMS-HIG-13-032

Search for two Higgs bosons in final states containing two photons and two bottom quarks in proton-proton collisions at 8 TeV

The CMS Collaboration*

Abstract

A search is presented for the production of two Higgs bosons in final states containing two photons and two bottom quarks. Both resonant and nonresonant hypotheses are investigated. The analyzed data correspond to an integrated luminosity of 19.7 fb^{-1} of proton-proton collisions at $\sqrt{s} = 8$ TeV collected with the CMS detector. Good agreement is observed between data and predictions of the standard model (SM). Upper limits are set at 95% confidence level on the production cross section of new particles and compared to the prediction for the existence of a warped extra dimension. When the decay to two Higgs bosons is kinematically allowed, assuming a mass scale $\Lambda_R = 1$ TeV for the model, the data exclude a radion scalar at masses below 980 GeV. The first Kaluza–Klein excitation mode of the graviton in the RS1 Randall–Sundrum model is excluded for masses between 325 and 450 GeV. An upper limit of 0.71 pb is set on the nonresonant two-Higgs boson cross section in the SM-like hypothesis. Limits are also derived on nonresonant production assuming anomalous Higgs boson couplings.

Published in Physical Review D as doi:10.1103/PhysRevD.94.052012.

*See Appendix A for the list of collaboration members

1 Introduction

The discovery of a boson with a mass of approximately 125 GeV, with properties close to those expected for the Higgs boson (H) of the standard model (SM) [1, 2], has stimulated interest in the exploration of the Higgs potential. The production of a pair of Higgs bosons (HH) is a rare process that is sensitive to the structure of this potential through the self-coupling mechanism of the Higgs boson. In the SM, the cross section for the production of two Higgs bosons in pp collisions at 8 TeV is 10.0 ± 1.4 fb for the gluon-gluon fusion process [3–5], which lies beyond the reach of analyses based on the first run of the CERN LHC.

Many theories beyond the SM (BSM) suggest the existence of heavy particles that can couple to a pair of Higgs bosons. These particles could appear as a resonant contribution in the invariant mass of the HH system. If the new particles are too heavy to be observed through a direct search, they may be sensed in the HH production through their virtual contributions (as shown, e.g., in Refs. [6, 7]); also, the fundamental couplings of the model can be modified relative to their SM values (as shown, e.g., in Refs. [8, 9]); in both cases, a nonresonant enhancement of the HH production could be observed.

Models with a warped extra dimension (WED), as proposed by Randall and Sundrum [10], postulate the existence of one spatial extra dimension compactified between two fixed points, commonly called branes. The region between the branes is referred to as bulk, and controlled through an exponential metric. The gap between the two fundamental scales of nature, such as the Planck scale (M_{Pl}), and the electroweak scale, is controlled by a warp factor (k) in the metric, which corresponds to one of the fundamental parameters of the model. The brane where the density of the extra dimensional metric is localized is called "Planck brane", while the other, where the Higgs field is localized, is called "TeV brane". This class of models predicts the existence of new particles that can decay to Higgs boson pair, such as the spin-0 radion [11–13], and the spin-2 first Kaluza–Klein (KK) excitation of the graviton [14–16].

There are two possible ways of describing a KK graviton in WED that depend on the choice of localization for the SM matter fields. In the RS1 model, only gravity is allowed to propagate in the extra-dimensional bulk. In this model the couplings of the KK-graviton to matter fields are controlled by $k/\overline{M}_{\mathrm{Pl}}$ [10], with the reduced Planck mass $\overline{M}_{\mathrm{Pl}}$ defined by $M_{\mathrm{Pl}}/\sqrt{8\pi}$. For the possibility of SM particles to propagate in the bulk (the so-called bulk-RS model), the coupling of the KK graviton to matter depends on the choice for the localization of the SM bulk fields. This paper uses the phenomenology of Ref. [17], where SM particles are allowed to propagate in the bulk, and follows the characteristics of the SM gauge group, with the right-handed top quark localized on the TeV brane (so called elementary top hypothesis).

The radion (R) is an additional element of WED models that is needed to stabilize the size of the extra dimension l. It is usual to express the benchmark points of the model in terms of the dimensionless quantity $k/\overline{M}_{\mathrm{Pl}}$, and the mass scale $\Lambda_{\mathrm{R}} = \sqrt{6}\exp[-kl]\overline{M}_{\mathrm{Pl}}$, with the latter interpreted as the ultraviolet cutoff of the model [18]. The addition of a scalar-curvature term can induce a mixing between the scalar radion and the Higgs boson [18, 19]. This possibility is discussed, for example, in Ref. [20]. Precision electroweak studies suggest that this mixing is expected to be small [21]. In our interpretations of the constraints we neglect the possibility of Higgs–radion mixing.

On one hand, the choice of localization of the SM matter fields for the KK-graviton resonance impacts the kinematics of the signal and drastically modifies the production and decay properties [22]. The physics of the radion, on the other hand, does not depend much on the choice of the model [18], which obviates the need to distinguish the RS1 and bulk-RS possibilities.

Models with an extended Higgs sector also predict one spin-0 resonance that, when sufficiently massive, decays to a pair of SM Higgs bosons, and would correspond to an additional Higgs boson. Examples of such models are the singlet extension [23], the two Higgs doublet models [24] (in particular the minimal supersymmetric model [25, 26]), and the Georgi-Machacek model [27]. The majority of these models predict that heavy scalar production occurs predominantly through the gluon-gluon fusion process. The Lorentz structure of the coupling between the scalar and the gluon is the same for a radion or a heavy Higgs boson. Therefore the models for the production of a radion or an additional Higgs boson are essentially the same, provided the interpretations are performed in a parameter space region where the spin-0 resonance is narrow. The results of this paper can therefore be easily applied to constrain this class of models.

Phenomenological explorations of the two-Higgs-boson channel were studied prior to the observation of the Higgs boson [28], and, since then, other studies have become available [29–35]. Most of these indicate that in BSM physics an enhancement of the HH production cross section is expected, together with modified signal kinematics for the HH final state. This paper describes a search for the production of pairs of Higgs bosons in the $\gamma\gamma\mathrm{b\bar{b}}$ final state in proton-proton (pp) collisions at the LHC, using data corresponding to an integrated luminosity of $19.7\,\mathrm{fb}^{-1}$ collected by the CMS experiment at $\sqrt{s} = 8\,\mathrm{TeV}$. Both nonresonant and resonant production are explored, with the search for a narrow resonance X conducted at masses m_X between 260 and 1100 GeV.

The fully-reconstructed $\gamma\gamma\mathrm{b\bar{b}}$ final state discussed in this paper, combines the large SM branching fraction ($\mathcal{B}$) of the $\mathrm{H} \to \mathrm{b\bar{b}}$ decay with the comparatively low background and good mass resolution of the $\mathrm{H} \to \gamma\gamma$ channel, yielding a total $\mathcal{B}(\mathrm{HH} \to \gamma\gamma\mathrm{b\bar{b}})$ of 0.26% [36]. The search exploits the mass spectra of the diphoton ($m_{\gamma\gamma}$), dijet (m_{jj}), and the four-body systems ($m_{\gamma\gamma\mathrm{jj}}$), as well as the direction of Higgs bosons in the Collins–Soper frame [37], to provide discrimination between production of two Higgs bosons and SM background.

A search in the same final state was performed by the ATLAS collaboration [38]. Complementary final states such as $\mathrm{HH} \to \mathrm{b\bar{b}b\bar{b}}$, $\mathrm{HH} \to \tau\tau\mathrm{b\bar{b}}$, and HH to multileptons and multiphotons were also explored by the ATLAS [39, 40] and CMS [41–44] collaborations.

This paper is organized as follows: Section 2 contains a brief description of the CMS detector. In Section 3 we describe the simulated signal and background event samples used in the analysis. Section 4 is dedicated to the discussion of event selection and Higgs boson reconstruction. The signal extraction procedure is discussed in Section 5. In Section 6 we present the systematic uncertainties impacting each analysis method. Section 7 contains the results of resonant and nonresonant searches, and Section 8 provides a summary.

2 The CMS detector

The CMS detector, its coordinate system, and main kinematic variables used in the analysis are described in detail in Ref. [45]. The detector is a multipurpose apparatus designed to study physics processes at large transverse momentum p_{T} in pp and heavy-ion collisions. The central feature of the apparatus is a superconducting solenoid, of 6 m internal diameter, providing a magnetic field of 3.8 T. A silicon pixel and strip tracker covering the pseudorapidity range $|\eta| < 2.5$, a crystal electromagnetic calorimeter (ECAL), and a brass and scintillator hadron calorimeter (HCAL) reside within the field volume. The ECAL is made of lead tungstate crystals, while the HCAL has layers of plates of brass and plastic scintillator. These calorimeters are both composed of a barrel and two endcap sections and provide coverage up to $|\eta| < 3.0$.

An iron and quartz-fibre Cherenkov hadron calorimeter covers larger values of $3.0 < |\eta| < 5.0$. Muons are measured in the $|\eta| < 2.4$ range, using detection planes based on three technologies: drift tubes, cathode strip chambers, and resistive-plate chambers.

The first level of the CMS trigger system, composed of special hardware processors, uses information from the calorimeters and muon detectors to select the most interesting events in a time interval of less than 4 μs. The high-level trigger (HLT) processor farm further decreases the event rate from around 100 kHz to less than 1 kHz, before data storage.

3 Simulated events

The MADGRAPH version 5.1.4.5 [46] Monte Carlo (MC) program generates parton-level signal events based on matrix element calculations at leading order (LO) in quantum chromodynamics (QCD), using LO PYTHIA version 6.426 [47] for showering and hadronization of partons. The models provide a description of production through gluon-gluon fusion of particles with narrow width (width set to 1 MeV) that decay to two Higgs bosons, with mass $m_{\mathrm{H}} = 125\,\mathrm{GeV}$, in agreement with Ref. [48]. Events are generated either for spin-0 radion production, or spin-2 KK-graviton production predicted by the bulk-RS model.

The samples for nonresonant production are generated considering the cross section dependence on three parameters: the Higgs boson trilinear coupling λ, parametrized as $\kappa_\lambda \equiv \lambda/\lambda^{\mathrm{SM}}$, where $\lambda^{\mathrm{SM}} \equiv m_{\mathrm{H}}^2/(2v^2) = 0.129$, with $v = 246\,\mathrm{GeV}$ being the vacuum expectation value of the Higgs boson; the top Yukawa coupling y_{t}, parametrized as $\kappa_{\mathrm{t}} \equiv y_{\mathrm{t}}/y_{\mathrm{t}}^{\mathrm{SM}}$, where $y_{\mathrm{t}}^{\mathrm{SM}} = m_{\mathrm{t}}/v$ is the SM value of the top Yukawa coupling, and m_{t} the top quark mass; and the coefficient c_2 of a possible coupling of two Higgs bosons to two top quarks. The first two parameters reflect changes relative to SM values, while the third corresponds purely to a BSM operator. In this parametrisation the SM production corresponds to the point $\kappa_\lambda = 1$, $\kappa_{\mathrm{t}} = 1$ and $c_2 = 0$. The parameters κ_λ and c_2 cannot be directly constrained by alternative measurements at the LHC. Therefore we vary these parameters in a wide range: $-20 \leq \kappa_\lambda \leq 20$ and $-3 \leq c_2 \leq 3$. The range $0.75 \leq \kappa_{\mathrm{t}} \leq 1.25$ is compatible with constraints from the single Higgs boson measurements provided in Ref. [49].

The part of the Higgs potential $\Delta\mathcal{L}$ relevant to two-Higgs boson production and their interactions with the top quark can be expressed as in Ref. [50]:

$$\Delta\mathcal{L} = \kappa_\lambda\,\lambda^{\mathrm{SM}} v\,H^3 - \frac{m_{\mathrm{t}}}{v}(v + \kappa_{\mathrm{t}}\,H + \frac{c_2}{v}HH)\,(\bar{t}_{\mathrm{L}}t_{\mathrm{R}} + \mathrm{h.c.}), \tag{1}$$

where t_{L} and t_{R} are the top quark fields with left and right chiralities, respectively, and H is the physical Higgs boson field.

Besides being used to predict SM single-Higgs boson production, the MC predictions for the background processes are used also in comparisons with data, to optimize the selection criteria, and for checking background-estimation methods based on control samples in data. The dominant background, originating from events with two prompt photons and two jets in the final state, is generated at next-to-leading-order (NLO) in QCD using SHERPA version 1.4.2 [51]. Multijet production with or without a single-prompt photon represents a subdominant background, and is generated with the PYTHIA 6 package. Other minor backgrounds, including Drell–Yan ($\mathrm{pp} \to \mathrm{Z}/\gamma^* \to \mathrm{e}^+\mathrm{e}^-$), SM Higgs boson production with jets, as well as vector boson and top quark production in association with photons, are generated using MADGRAPH and PYTHIA 6, or the generator POWHEG version 1.0 [52–54] at NLO in QCD. The generated events are processed through GEANT4-based [55, 56] detector simulation.

4 Event reconstruction

The events are selected using two complementary HLT paths requiring two photons. The first trigger requires an identification based on the energy distribution of the electromagnetic shower and loose isolation requirements on photon candidates. The second trigger applies tighter constraints on the shower shape, but a looser kinematic selection. The trigger thresholds on the p_T range between 26 and 36 GeV, and between 18 and 22 GeV, respectively, for photons with highest (leading) and next-to-highest (subleading) p_T, with specific choices that depend on the instantaneous LHC luminosity. The HLT paths are more than 99% efficient for the selection criteria used in this analysis [57].

4.1 The $H \to \gamma\gamma$ candidate

Photon candidates are constructed from clusters of energy in the ECAL [58, 59]. They are subsequently calibrated [60] and identified through a cutoff-based approach (referred to as "cut-based analysis" in Ref. [57]). The identification criteria include requirements on p_T of the electromagnetic shower, its longitudinal leakage into the HCAL, its isolation from jet activity in the event, as well as a veto on the presence of a track matching the ECAL cluster. These criteria provide efficient rejection of objects that arise from jets or electrons but are reconstructed as photons. Both photons are required to be within the ECAL fiducial volume of $|\eta_\gamma| < 2.5$. Small transition regions between the ECAL barrel and the ECAL endcaps are excluded in this analysis, because the reconstruction of a photon object in this region is not optimal.

The directions of the photons are reconstructed assuming that they arise from the primary vertex of the hard interaction. However on average ≈20 additional pp interactions (pileup) occur in the same or neighboring pp bunch crossings as the main interaction. Many additional vertexes are therefore usually reconstructed in an event using charged particle tracks. We assume that the primary interaction vertex corresponds to the one that maximizes the sum in p_T^2 of the associated charged particle tracks. For the simulated signal, it is shown that this choice of vertex lies within 1 cm of the true hard-interaction vertex in 99% of the events. With this choice for energy reconstruction and vertex identification, the diphoton mass resolution remains close to 1 GeV independent of the signal hypothesis.

Diphoton candidates are preselected by requiring $100 < m_{\gamma\gamma} < 180$ GeV. The two photons are further required to satisfy the asymmetric selection criteria $p_T^{\gamma 1}/m_{\gamma\gamma} > 1/3$ and $p_T^{\gamma 2}/m_{\gamma\gamma} > 1/4$, where $p_T^{\gamma 1}$ and $p_T^{\gamma 2}$ are the transverse momenta of the leading and subleading photons. The use of different p_T thresholds scaled by the diphoton invariant mass, minimizes turn-on effects that can distort the distribution at the low-mass end of the $m_{\gamma\gamma}$ spectrum. If there is more than one diphoton candidate selected through the above requirements, the pair with the largest scalar sum in the p_T of the two photons is chosen for analysis.

4.2 The $H \to b\bar{b}$ candidate

The Higgs boson candidate decaying into two b quarks is reconstructed following a procedure similar to that used in CMS searches for SM Higgs bosons that decay to b quarks [61].

The particle-flow event algorithm reconstructs and identifies each individual particle (referred to as candidates) with an optimized combination of information from the various elements of the CMS detector [62, 63]. Then, the anti-k_T algorithm [64] clusters particle-flow candidates into jets using a distance parameter $D = 0.5$. Jets are required to be within the tracker acceptance ($|\eta_j| < 2.4$), and separated from both photons through a condition on the angular distance in $\eta \times \phi$ space of $\Delta R_{\gamma j} \equiv \sqrt{(\Delta\eta)^2 + (\Delta\phi)^2} > 0.5$, where ϕ is the azimuth angle in radians.

The jet energy is corrected for extra depositions from pileup interactions, using the jet-area technique [65] implemented in the FASTJET package [66]. Jet energy corrections are applied as a function of η_j and p_T^j [67, 68]. Identification criteria are applied to reject detector noise misidentified as jets, and the procedure is verified using simulated signal.

The identification of jets likely to have originated from hadronization of b quarks exploits the combined secondary vertex (CSV) b quark tagger [69]. This algorithm combines the information from track impact parameters and secondary vertexes within a given jet into a continuous output discriminant. Jets with CSV tagger values above some fixed threshold are considered as b tagged. The working point chosen in this analysis corresponds to an efficiency, estimated from simulated multijet events, of ≈70% and a mistag rate for light quarks and gluons of 1–2%, depending on jet p_T. This efficiency and the mistag rate are measured in data samples enriched in b jets (e.g., in $t\bar{t}$ events). Correction factors of ≈ 0.95 are determined from data-to-simulation comparisons and applied as weights to all simulated events.

Events are kept if at least two jets are selected and at least one of them is b tagged. To improve signal sensitivity, events are subsequently classified in two categories: events with exactly one b-tagged jet (medium purity) and events with more than one b-tagged jet (high purity). In the former category, the $H \to b\bar{b}$ decay is reconstructed by pairing the b-tagged jet with a non b-tagged jet, while in the latter category a pair of b-tagged jets is used. In both cases, when multiple pairing possibilities exist for the Higgs boson candidate, the dijet system with largest p_T is retained for further study. For medium- and high-purity simulated signal events, this procedure selects the correct jets in more than 80% and more than 95%, respectively.

The resolution in m_{jj} improves from 20 GeV for $m_X = 300$ GeV to 15 GeV for $m_X = 1$ TeV in the high-purity category, and from 25 GeV for $m_X = 300$ GeV to 15 GeV for $m_X = 1$ TeV in the medium-purity category. In the search for a low-mass resonance, the dijet mass resolution is improved using a multivariate regression technique [61] that uses the global information from the events as well as the particular properties of each jet, in an attempt to identify the semileptonic decays of B mesons and correct for the energy carried away by undetected neutrinos. The relative improvement in resolution is typically 15%. For the high mass analysis and nonresonant analysis the m_{jj} resolution is better than for low mass analysis. The improvement provided by the regression technique was found to be very limited. Therefore in those cases no regression was used.

Independent of whether a search involves the usage of jet energy regression, all jets are required to have $p_T^j > 25$ GeV. Finally, we require that $60 < m_{jj} < 180$ GeV.

4.3 The two-Higgs-boson system

The object selections discussed thus far are summarized in Table 1.

In each category, two Higgs bosons are obtained by combining the diphoton and the dijet boson candidates. To improve the resolution in $m_{\gamma\gamma jj}$, an additional constraint is imposed requiring m_{jj} to be consistent with m_H. This is achieved by modifying the jet 4-momenta using multiplicative factors. The value of each factor is obtained event-by-event through a χ^2 minimization procedure where the size of the denominator is defined by the estimated resolution for each jet [70]. The procedure, similar to the one used in Ref. [70], is referred to as a kinematic fit and the resulting four-body mass is termed $m_{\gamma\gamma jj}^{kin}$.

The scattering angle, θ_{HH}^{CS}, is defined in the Collins–Soper frame of the four-body system state, as the angle between the momentum of the Higgs boson decaying into two photons and the

Table 1: Summary of the analysis preselections.

Photons		Jets	
Variable	Range	Variable	Range
$p_{\mathrm{T}}^{\gamma 1}/m_{\gamma\gamma}$	$>1/3$	$p_{\mathrm{T}}^{\mathrm{j}}$ (GeV)	>25
$p_{\mathrm{T}}^{\gamma 2}/m_{\gamma\gamma}$	$>1/4$		
$\lvert\eta_{\gamma}\rvert$	<2.5	$\lvert\eta_{\mathrm{j}}\rvert$	<2.4
$m_{\gamma\gamma}$ (GeV)	$[100, 180]$	m_{jj} (GeV)	$[60, 180]$
		b-tagged jets	>0

line that bisects the acute angle between the colliding protons. In the Collins–Soper frame, the two Higgs boson candidates are collinear, and the choice of the one decaying to photons as reference is therefore arbitrary. Using the absolute value of the cosine of this angle, $\left|\cos\theta_{\mathrm{HH}}^{\mathrm{CS}}\right|$, obviates this arbitrariness.

4.4 Backgrounds

The SM background in $m_{\gamma\gamma}$ can be classified into two categories: the nonresonant background, from multijet and electroweak processes, and a peaking background corresponding to events from single-Higgs bosons decaying to two photons.

After the baseline selections of Table 1, the dominant nonresonant background with two prompt photons and more than two extra jets, referred to as $\gamma\gamma + \geq$2 jets, represents $\approx$75% of the total background. The nonresonant background with one prompt photon and a jet misidentified as a photon as well as more than two extra jets, referred to as γ jet$+ \geq 2$ jets, represents in turn $\approx$ 25%. The background from two jets misidentified as photons is negligible.

The remaining nonresonant and resonant backgrounds contribute much less than 1% to the total. They represent associated production of photons with top quarks or single electroweak bosons decaying to quarks, and Drell–Yan events with their decay electrons misidentified as photons. The resonant backgrounds correspond to different SM processes contributing to single-Higgs boson production.

All nonresonant backgrounds are estimated from data, and the resonant background from SM single-Higgs boson production in different channels is taken from the MC simulation normalized to NLO or next-to-NLO (NNLO) production cross sections, whichever are available [36].

The comparison between data and MC predictions is provided in Fig. 1. The $\gamma\gamma/\gamma$ jet $+ \geq$2 jets background is normalized to the total integral of data in the signal free region, defined by the condition $m_{\gamma\gamma} > 130$ or $m_{\gamma\gamma} < 120$ GeV in addition to the selections of Table 1.

5 Analysis methods

In the final step, this analysis exploits kinematic properties of the final state to discriminate either resonant or nonresonant signal from SM background: the Higgs boson masses $m_{\gamma\gamma}$ and m_{jj}, the cosine of their scattering angle $\left|\cos\theta_{\mathrm{HH}}^{\mathrm{CS}}\right|$, and the mass of the two-Higgs-boson system, $m_{\gamma\gamma\mathrm{jj}}^{\mathrm{kin}}$. Distributions in these variables are shown for different signal assumptions in Fig. 2. The signal peaks in $m_{\gamma\gamma}$ and m_{jj} are shown in Figs. 2(a) and (b). The corresponding distributions for the QCD background are smoothly varying over the shown ranges. The $\left|\cos\theta_{\mathrm{HH}}^{\mathrm{CS}}\right|$ is rather

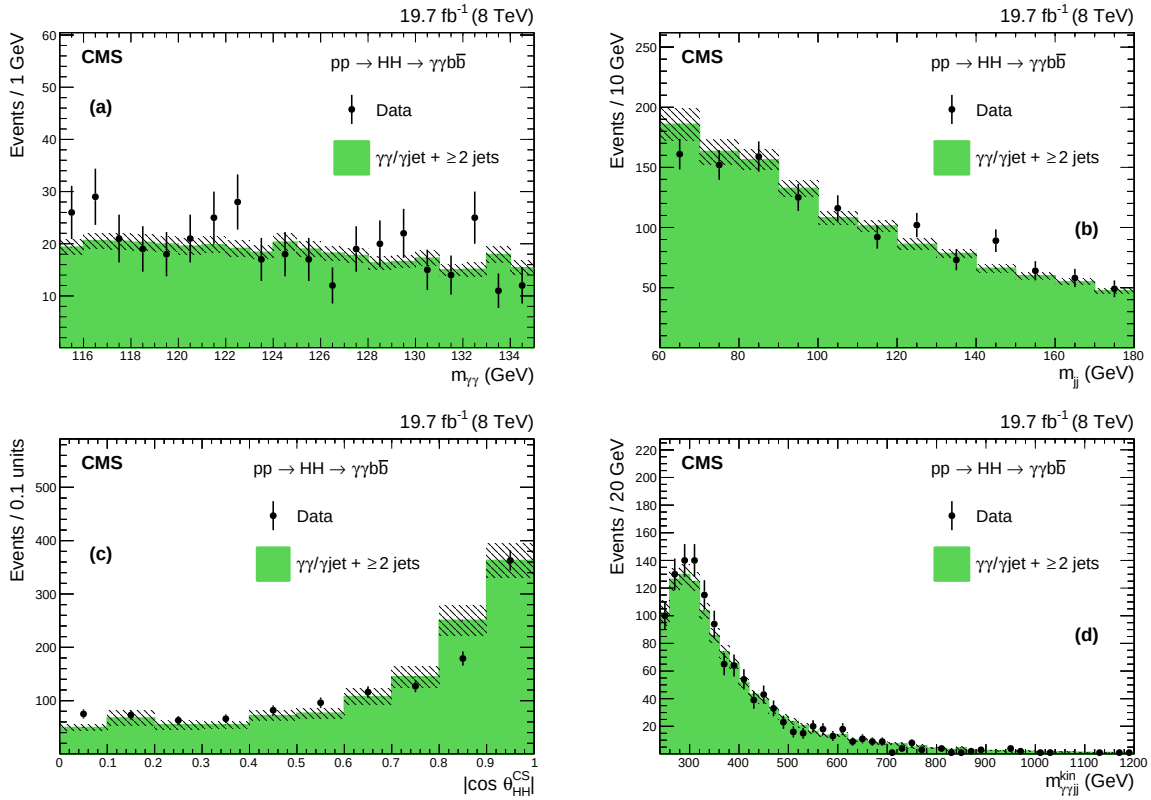

Figure 1: Reconstructed spectra for data compared to the $\gamma\gamma/\gamma\,\text{jet} + \geq 2\,\text{jets}$ background after the selections described in Table 1 (selections on photons and jets and a requirement of at least one b-tagged jet): (a) $m_{\gamma\gamma}$, (b) m_{jj}, (c) $\left|\cos\theta^{CS}_{HH}\right|$, and (d) $m^{kin}_{\gamma\gamma jj}$. The hatched area corresponds to the bin-by-bin statistical uncertainties on the background prediction reflecting the limited size of the generated MC sample. The comparison is provided for illustrative purpose, in the backgrounds, except the one coming from single-Higgs production, are evaluated from a fit to the data without reference to the MC simulation.

uniform for signal, as shown in Fig. 2(c), while it peaks toward one for background. Finally, a resonant signal appears as a narrow peak in $m^{kin}_{\gamma\gamma jj}$ spectrum, while the nonresonant signal has a broad contribution as shown in Fig. 2(d).

The dominant background from non-resonant production of prompt photons and jets exhibits a kinematic peak around $m^{kin}_{\gamma\gamma jj} \approx 300\,\text{GeV}$ followed by a slowly falling tail at high $m^{kin}_{\gamma\gamma jj}$. In the resonant case, we consider two strategies, one for m_X close to the kinematic peak, and one for m_X heavier than the kinematic peak. A third strategy is considered for the nonresonant case, since the signal distribution as function of $m^{kin}_{\gamma\gamma jj}$ is broad. In all cases a categorization is used based on the number of b-tagged jets. All the strategies are summarized in Table 2 and briefly described below:

1. Resonant search in the low-mass region ($260 \leq m_X \leq 400\,\text{GeV}$): the events are selected in a narrow window around the m_X hypothesis in the $m^{kin}_{\gamma\gamma jj}$ spectrum, and the signal is identified simultaneously in the $m_{\gamma\gamma}$ and m_{jj} spectra. This approach avoids a direct search for a resonance in the $m^{kin}_{\gamma\gamma jj}$ spectrum near the top of the kinematic peak of the SM background.

2. Resonant search in the high-mass region ($400 \leq m_X \leq 1100\,\text{GeV}$): the events are selected

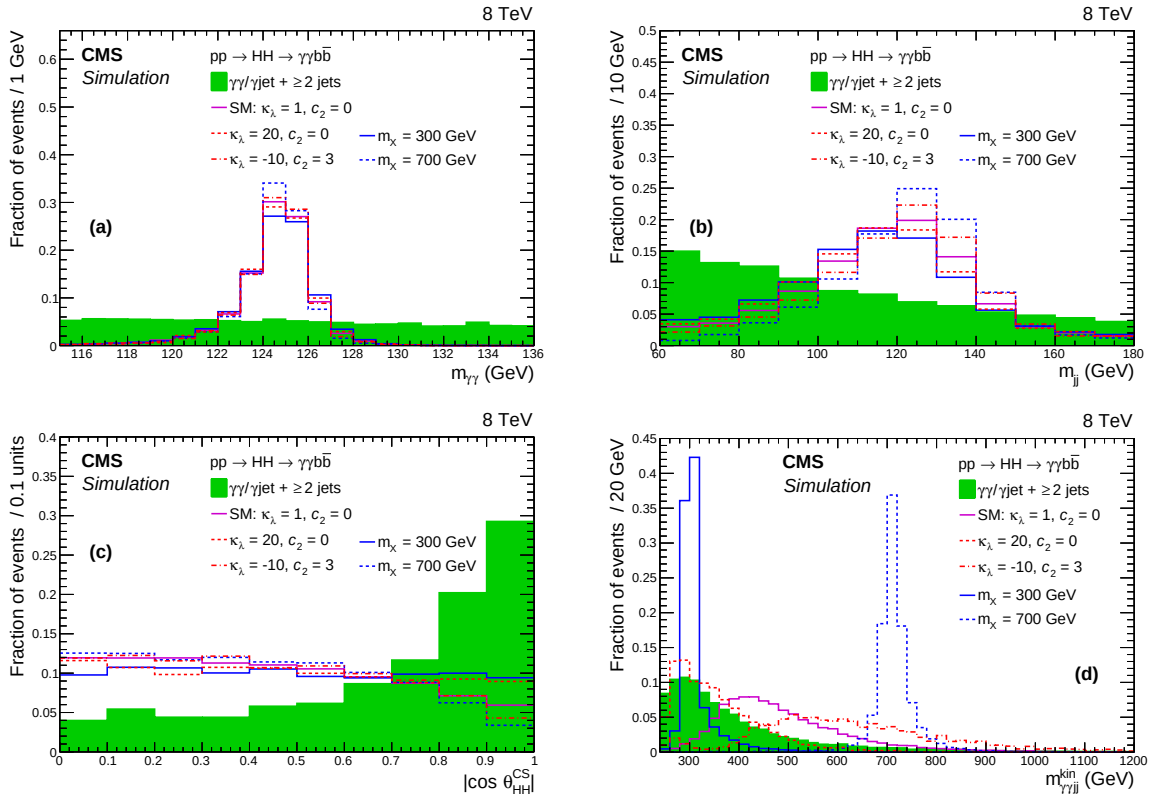

Figure 2: Simulated spectra for the spin-0 radion signal at $m_X = 300$ and 700 GeV, and for some values of the anomalous couplings, compared to SM Higgs boson production and QCD background, after the selections described in Table 1 (selections on photons and jets and a requirement of at least one b-tagged jet): (a) $m_{\gamma\gamma}$, (b) m_{jj}, (c) $|\cos\theta^{CS}_{HH}|$, and (d) $m^{kin}_{\gamma\gamma jj}$. All spectra are normalized to unity.

in a window around m_H in both the $m_{\gamma\gamma}$ and m_{jj} spectra, and the signal is identified in the $m^{kin}_{\gamma\gamma jj}$ spectrum.

3. Nonresonant search: a selection is applied in the $|\cos\theta^{CS}_{HH}|$ variable to reduce the background. In addition to the categorization in the number of b-tagged jets, a categorization is applied in $m^{kin}_{\gamma\gamma jj}$ by defining a high-mass region and a low-mass region. The signal is identified simultaneously in the $m_{\gamma\gamma}$ and m_{jj} spectra.

Table 2: Summary of the search analysis methods.

Signal hypothesis	Select	# categories	Fit
(1) $m_X \leq 400$ GeV	$m^{kin}_{\gamma\gamma jj}$	2 (b tags)	$m_{\gamma\gamma}$, m_{jj}
(2) $m_X \geq 400$ GeV	$m_{\gamma\gamma}$, m_{jj}	2 (b tags)	$m^{kin}_{\gamma\gamma jj}$
(3) Nonresonant	$\|\cos\theta^{CS}_{HH}\|$	4 (b tags, $m^{kin}_{\gamma\gamma jj}$)	$m_{\gamma\gamma}$, m_{jj}

The nonresonant background is described through different functions such as exponentials, power-law, or polynomials in the Bernstein basis [57]. When the search is performed simultaneously in the diphoton and dijet mass spectra, these functions are used to construct a two-dimensional (2D) probability density (PD) for the background in each category, following an approach similar to Ref. [71]. Otherwise, a one-dimensional (1D) PD is used. In all cases, we

choose the background PD to minimize the bias on signal. The bias is always found to be at least a factor of 7 smaller than the statistical uncertainty in the fit, and can be safely neglected [1].

In each invariant mass distribution used to identify the signal, the signal PD is modeled, following the same approach as in Ref. [57], through the sum of a Gaussian function and a Crystal Ball (CB) function [72], using the parameters extracted from fits to MC simulations. The resolution parameters in both functions are kept independent, $\sigma_{\mathrm{x}}^{\mathrm{G}}$ for the Gaussian and $\sigma_{\mathrm{x}}^{\mathrm{CB}}$ for the CB function, but in the fits to each of the channels ($\mathrm{x} = \gamma\gamma$, jj, $\gamma\gamma$jj), we let the μ parameter for both the Gaussian and the CB component float, which provides three independent μ_{x} values.

Finally, we consider the contribution from SM single-Higgs boson production in 2D searches. The gluon-gluon and vector-boson fusion processes are modeled in $m_{\gamma\gamma}$ by a sum over Gaussian and CB functions, and through a constant term in m_{jj}. The associated production of vector bosons that subsequently decay to jets, and the SM single-Higgs bosons are modeled in the same way as the signal. The parameters of the distribution are extracted from a fit to the MC simulation.

The total PD used for signal extraction corresponds to a sum over separate PD contributions from the signal component, single-Higgs boson production, and nonresonant backgrounds. We also verify that 2D PD functions can be considered as uncorrelated between $m_{\gamma\gamma}$ and m_{jj} within the statistical uncertainties. To obtain this result we calculated the correlation in data. The uncertainty in the correlation was estimated by generating pseudo-experiments from a model assuming no correlation between $m_{\gamma\gamma}$ and m_{jj} and calculating the root mean square of the resulting distribution.

5.1 Low-mass resonant

In addition to the preselections summarized in Table 1, each mass hypothesis has a selection applied on $m_{\gamma\gamma\mathrm{jj}}^{\mathrm{kin}}$ in a narrow window around m_{X}. The window sizes increase with m_{X} to account for the increasing experimental resolution from $\Delta m_{\mathrm{X}} = \pm 10\,\mathrm{GeV}$ at $m_{\mathrm{X}} = 260\,\mathrm{GeV}$ to $\Delta m_{\mathrm{X}} = ^{+31}_{-20}$ GeV at $m_{\mathrm{X}} = 400\,\mathrm{GeV}$.

A possible signal can be extracted from data using a simultaneous fit to the $m_{\gamma\gamma}$ and m_{jj} spectra. The sensitivity to the signal in this search is increased through the b jet energy regression that improves the resolution of the signal in m_{jj}. The background-only PD is a first-order polynomial in the Bernstein basis and a power law in the medium- and high-purity categories, respectively, as shown in Fig. 3, together with their 68% and 95% confidence level (CL) contours for the selection optimized for the search with $m_{\mathrm{X}} = 300\,\mathrm{GeV}$, $290 < m_{\gamma\gamma\mathrm{jj}}^{\mathrm{kin}} < 310\,\mathrm{GeV}$.

As a cross-check, two alternative signal extraction techniques are tested. In one, a selection is performed in the m_{jj} spectrum, and the signal extracted in the $m_{\gamma\gamma}$ spectrum. In the other, a selection is performed in the m_{jj} spectrum and the $m_{\gamma\gamma\mathrm{jj}}$ spectrum is exploited, using a normalization extracted from sidebands in the $m_{\gamma\gamma}$ spectrum. The two procedures give compatible results within the statistical uncertainties.

5.2 High-mass resonant

In addition to the requirements in Table 1, selections are applied on $m_{\gamma\gamma}$ and m_{jj}, as summarized in Table 3.

A possible signal can be extracted from a fit to the $m_{\gamma\gamma\mathrm{jj}}^{\mathrm{kin}}$ distribution for mass points between $320 \leq m_{\gamma\gamma\mathrm{jj}}^{\mathrm{kin}} \leq 1200\,\mathrm{GeV}$. The background-only PD is a power law for each category, and is seen to well describe the data in Fig. 4. The lower threshold of 320 GeV is chosen to avoid the

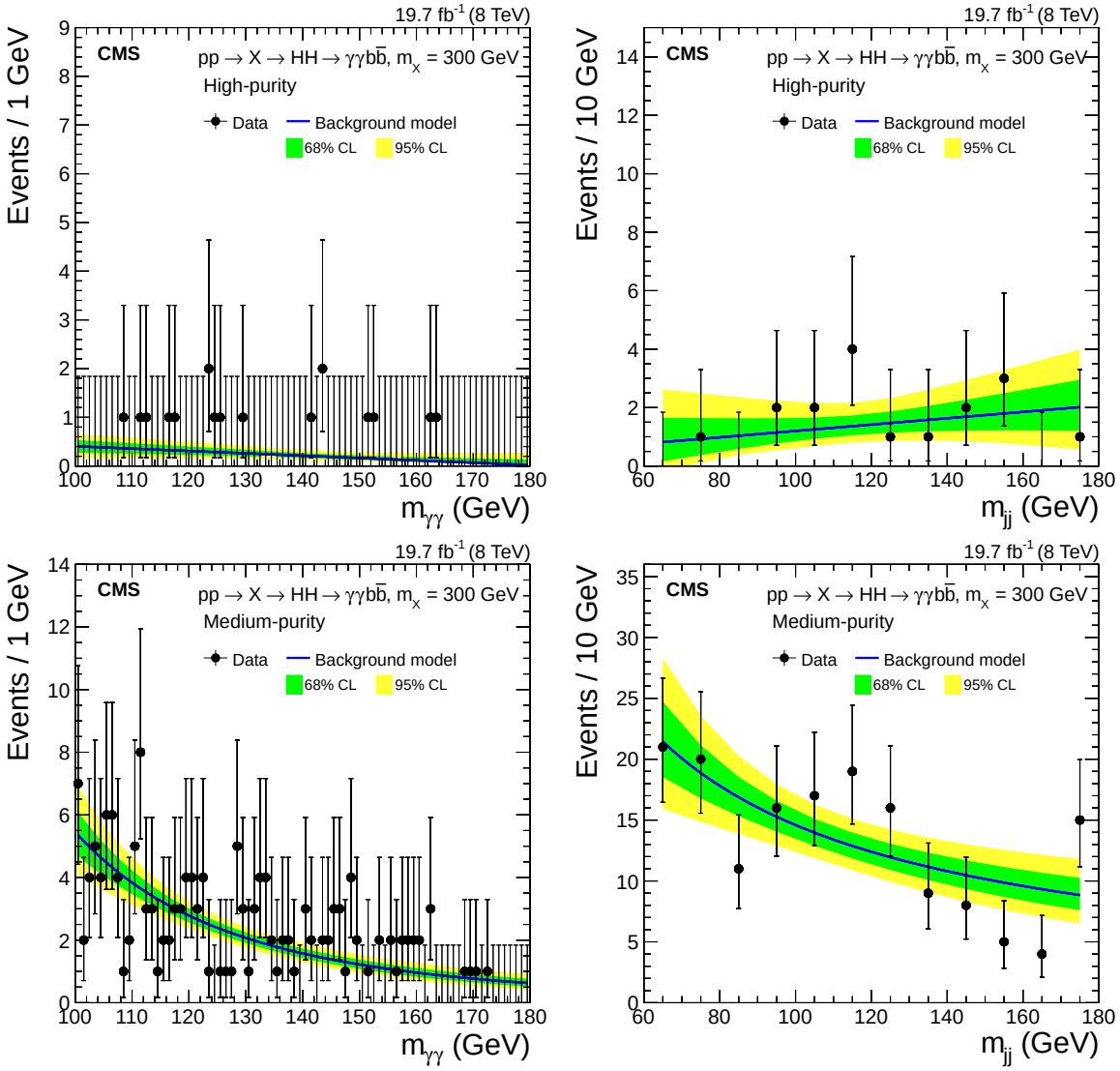

Figure 3: Low-mass resonant analysis: fits to the nonresonant background contribution in high-purity category to the $m_{\gamma\gamma}$ (top-left) and m_{jj} spectra (top-right), and similarly for medium-purity category in bottom-left and bottom-right, respectively. The fits to the background-only hypothesis are given by the blue curves, along with their 68% and 95% CL contours. The selections are designed to search for a $m_X = 300\,\text{GeV}$ hypothesis: $290 < m^{\text{kin}}_{\gamma\gamma jj} < 310\,\text{GeV}$.

kinematic turn-on, while still ensuring full containment of signal for the $m_X \geq 400\,\text{GeV}$ mass hypotheses. Single-Higgs boson production is a negligible background in this phase space region, and is absorbed into the parametrization of the nonresonant background.

5.3 Nonresonant

We apply a selection on $|\cos\theta^{\text{CS}}_{\text{HH}}|$ in the search for nonresonant two-Higgs boson production. To increase the sensitivity to a large variety of BSM topologies (see examples shown in Fig. 2), an additional categorization is applied in $m^{\text{kin}}_{\gamma\gamma jj}$. For the SM-like topology in gg $\rightarrow$ HH production, the $m^{\text{kin}}_{\gamma\gamma jj}$ spectrum peaks roughly at 400 GeV, while for $|\kappa_\lambda| \gtrsim 10$ the peak shifts down to the kinematic threshold of $m^{\text{kin}}_{\gamma\gamma jj} \approx 250\,\text{GeV}$. Large absolute values of the c_2 ($|c_2| \approx 3$) parameter usually lead to an opposite effect by shifting the peak in $m^{\text{kin}}_{\gamma\gamma jj}$ spectrum above 400 GeV. Two

Table 3: Additional selection criteria applied in the high-mass resonant search.

Variable	Range (GeV)	
	Medium-purity	High-purity
$m_{\gamma\gamma}$	122–128	120–130
m_{jj}	85–170	

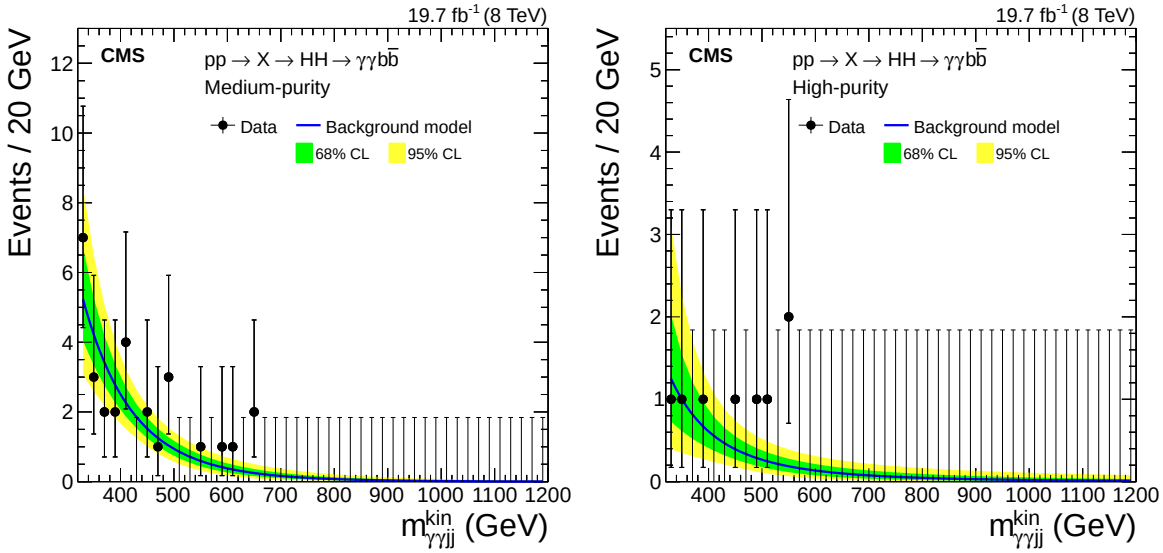

Figure 4: High-mass resonant analysis: fits to the nonresonant background contribution to the $m^{\mathrm{kin}}_{\gamma\gamma\mathrm{jj}}$ spectrum in medium- (left) and in high-purity (right) events. The fits to the background-only hypothesis are given by the blue curves, along with their 68% and 95% CL contours.

categories are defined for $m^{\mathrm{kin}}_{\gamma\gamma\mathrm{jj}}$ smaller or larger than 350 GeV, a value optimized for SM-like search. The details of the selections and categorizations are provided in Table 4.

A possible signal can be extracted using a simultaneous fit to the $m_{\gamma\gamma}$ and m_{jj} spectra. The background-only PD are exponentials and power-law expressions for the medium- and high-purity categories, respectively, which agree with the data, as can be seen in Figs. 5 and 6.

Table 4: Additional selections applied in the nonresonant searches.

Variable	High-purity		Medium-purity	
$\lvert\cos\theta^{\mathrm{CS}}_{\mathrm{HH}}\rvert$	<0.9		<0.65	
$m^{\mathrm{kin}}_{\gamma\gamma\mathrm{jj}}$ categorization (GeV)	<350	>350	<350	>350

5.4 Signal efficiency

The signal efficiency is a function of the mass hypothesis, as shown in Fig. 7. It is estimated with respect to all events generated in a given signal sample. The efficiency increases as the resonance mass increases from $m_X = 260$ to 900 GeV because of higher photon and jet reconstruction efficiencies. The efficiency starts to drop for $m_X > 900$ GeV. At this point, the typical angular distance in the laboratory frame between two b quarks produced in Higgs boson decay is of the order of the distance parameter D [73]. The minimum in efficiency is observed at $m_X = 300$ GeV. It results from an optimization procedure designed to maximize the overall analysis sensitivity. This procedure chooses an optimal size of $m^{\mathrm{kin}}_{\gamma\gamma\mathrm{jj}}$ window for each m_X hypothesis. For $m_X = 300$ GeV, the background is largest and the resulting $m^{\mathrm{kin}}_{\gamma\gamma\mathrm{jj}}$ window is

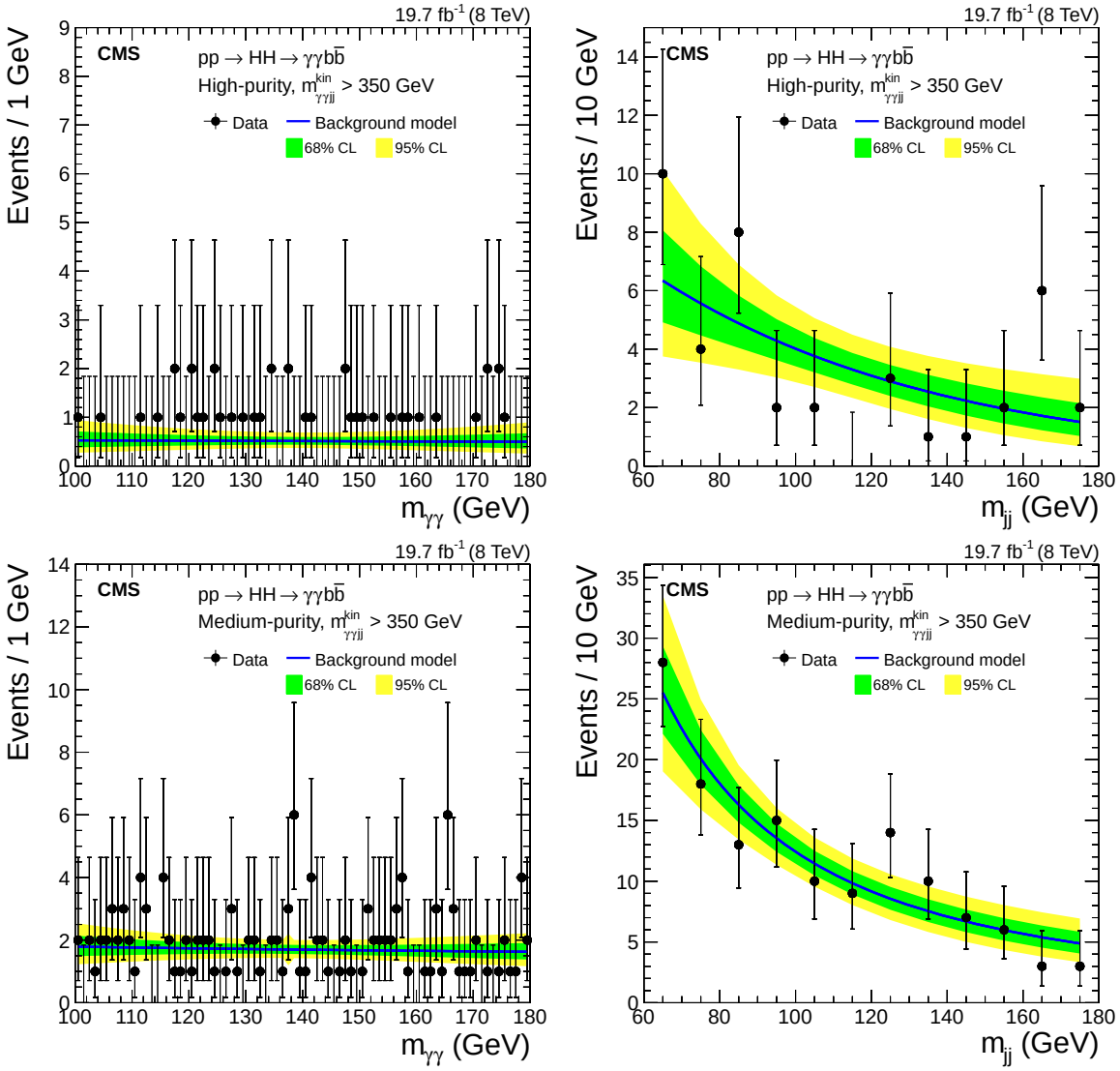

Figure 5: Nonresonant analysis: fits to the nonresonant background contribution in high-$m^{\text{kin}}_{\gamma\gamma\text{jj}}$ and high-purity category to the $m_{\gamma\gamma}$ (top-left) and m_{jj} spectra (top-right), and similarly for medium-purity category in bottom-left and bottom-right, respectively. The fits to the background-only hypothesis are given by the blue curves, along with their 68% and 95% CL contours.

smallest, inducing a small drop in signal selection efficiency. Finally, the single and double b tag categories contribute in roughly equal ways to the total efficiency.

Figure 8 provides the efficiencies of selecting the signal events as function of κ_λ for different values of κ_t and assuming $c_2 = 0$. The left plot provides efficiencies for $m^{\text{kin}}_{\gamma\gamma\text{jj}} < 350\,\text{GeV}$ categories and right for $m^{\text{kin}}_{\gamma\gamma\text{jj}} > 350\,\text{GeV}$ categories. For large values of $|\kappa_\lambda|$ (typically larger than 10) the efficiency is rather flat, while for small values of $|\kappa_\lambda|$ the efficiency in the $m^{\text{kin}}_{\gamma\gamma\text{jj}} < 350\,\text{GeV}$ ($m^{\text{kin}}_{\gamma\gamma\text{jj}} > 350\,\text{GeV}$) categories is reduced (increased). The change in efficiency is caused by the interference between two-Higgs box diagrams and the Higgs self coupling channel. The total efficiency in four categories is ≈15–30%, depending on the model parameters. This figure illustrates the way that $m_{\gamma\gamma\text{jj}}$ categorization can help separate different nonresonant signal hypotheses.

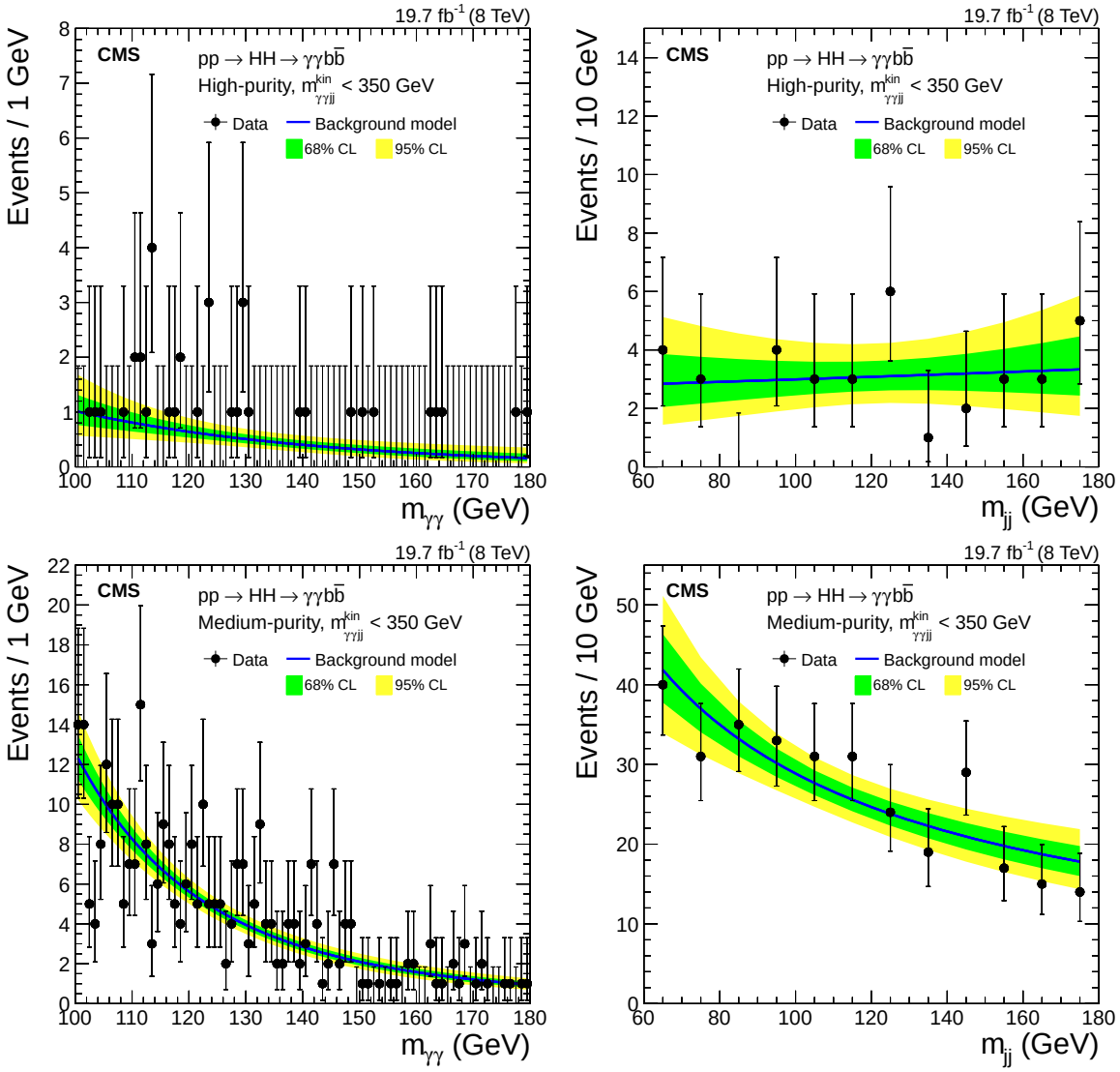

Figure 6: Nonresonant analysis: fits to the nonresonant background contribution in low-$m^{\text{kin}}_{\gamma\gamma\text{jj}}$ and high-purity category to the $m_{\gamma\gamma}$ (top-left) and m_{jj} spectra (top-right), and similarly for medium-purity category in bottom-left and bottom-right, respectively. The fits to the background-only hypothesis are given by the blue curves, along with their 68% and 95% CL contours.

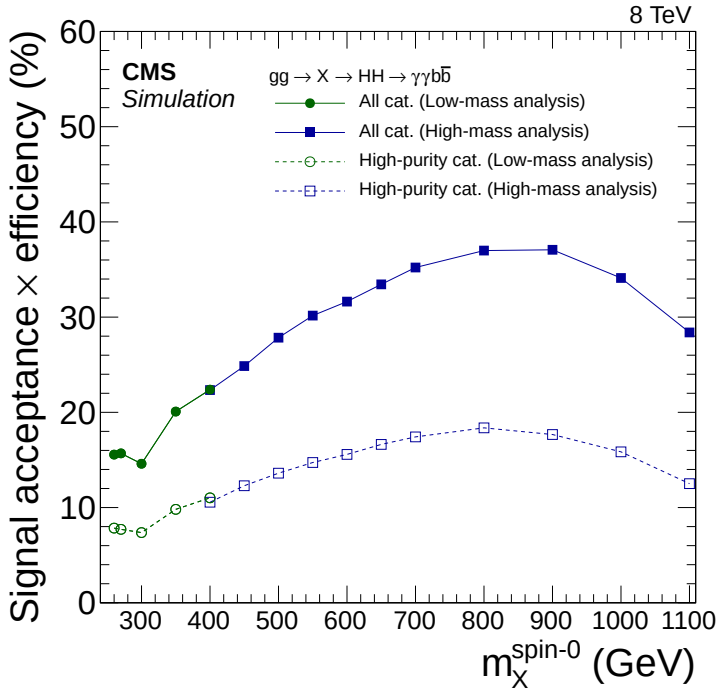

Figure 7: Resonant signal efficiency for the final selection described in Table 1 and Section 5. The efficiency is shown for a spin-0 hypothesis of a radion particle, but is similar for a spin-2 hypothesis of a KK graviton. The error bars associated with statistical uncertainties are smaller than the size of the markers.

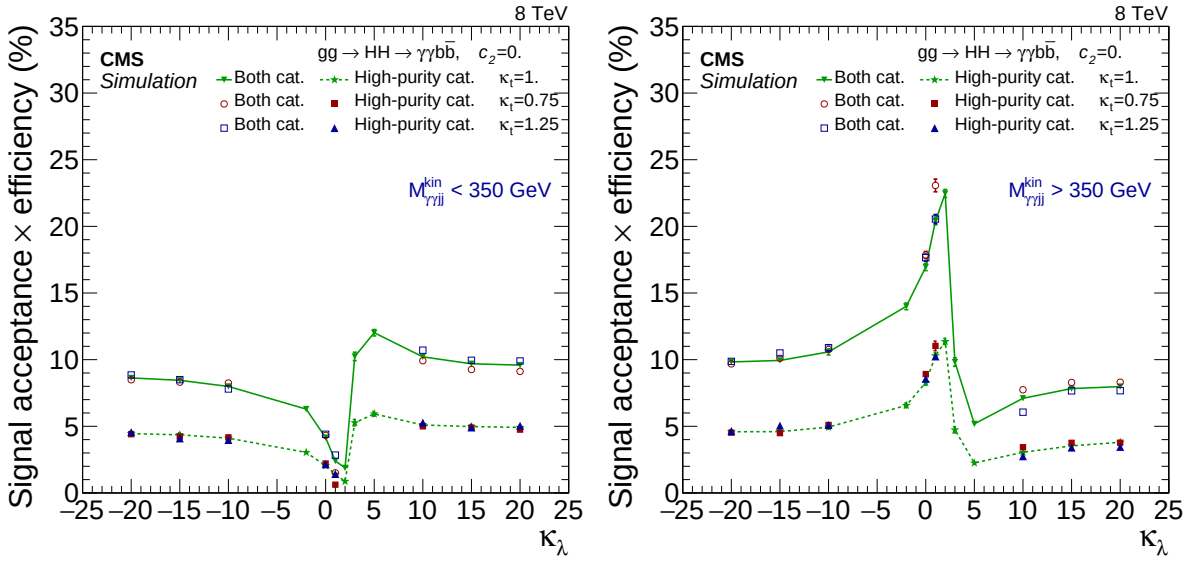

Figure 8: Signal efficiency for $c_2 = 0$ as function of κ_λ for different values of κ_t, for the low-$m^{\text{kin}}_{\gamma\gamma\text{jj}}$ region (left) and high-$m^{\text{kin}}_{\gamma\gamma\text{jj}}$ region (right).

6 Systematic uncertainties

The analysis defines a likelihood function based on the total PD and the data. The parameters for total signal and for the background-only PD are constrained in the fit to maximize this function. A uniform prior is used to parametrize the background PD. When converting the fitted yields into production cross sections, we use simulations to estimate the selection efficiency for the signal. The difference between the simulation and the data is corrected through scaling factors. The uncertainty in those factors is taken into account through parameters included in the likelihood function. The nuisance parameters (parameters not of immediate interest) are varied in the fit according to a log-normal probability density function. They can be classified into three categories. The first category contains the uncertainty in the estimation of the integrated luminosity, which is taken as 2.6% [74]. The second category includes systematic uncertainties that modify the efficiency of signal selection. Finally the third category contains the uncertainties that impact the signal or the Higgs boson PD. More precisely, the values of the PD parameters are taken from fits to the MC simulation of signal and Higgs boson production. The systematic uncertainties affect the mean values and the resolution parameters of the PD, while all other CB parameters are fixed to their best values. The sources of nuisance parameters are described below and their contribution to different categories are presented in Table 5.

The photon-related uncertainties are discussed in Ref. [57]. While the photon energy scale (PES) is known at the sub-percent level in the region of p_{T}^{γ} characteristic of the SM $\mathrm{H} \to \gamma\gamma$ signal, the uncertainty increases to 1% for $p_{\mathrm{T}}^{\gamma} > 100\,\mathrm{GeV}$. The photon energy resolution (PER) is known with a 5% precision [57]. A 1% normalization uncertainty is estimated in the offline diphoton selection efficiency and in the trigger efficiency. An additional normalization uncertainty of 5% is estimated for the high-mass region to account for differences in the p_{T} spectrum of signal photons and of electrons from $\mathrm{Z} \to \mathrm{ee}$ production used to estimate the quoted uncertainties.

The uncertainty in the jet energy scale (JES) is accounted for by changing the jet response by 1–2% [68], depending on the kinematics, while the uncertainty in the jet energy resolution (JER) is estimated by changing the jet resolution by 10% [67]. An additional 1% uncertainty in the four-body mass accounts for effects in the high-mass region related to the partial overlap between the two b jets from the Higgs boson decay. The uncertainty in the b tagging efficiency is estimated by changing the b tagging scale factor up and down by one standard deviation in each purity category [69]. The related systematic uncertainties are known to be anticorrelated between the two categories.

Theoretical systematic uncertainties are considered for the single-Higgs boson contribution from SM production, corresponding to the scale dependence of higher-order terms and impact from the choice of proton parton distribution functions (PDF) [36, 75]. No theoretical uncertainties are assumed on BSM signals. However, there is one exception. We consider the situation where the kinematic properties of the new signal are identical to those of the SM, but the cross section is different (SM-like search). In that case we parametrize the BSM cross section $\sigma_{\mathrm{HH}}^{\mathrm{BSM}}$ by the ratio $\mu_{\mathrm{HH}} = \sigma_{\mathrm{HH}}^{\mathrm{BSM}}/\sigma_{\mathrm{HH}}^{\mathrm{SM}}$. When such a search is performed the theoretical uncertainties on $\sigma_{\mathrm{HH}}^{\mathrm{SM}}$ are included in the likelihood. Finally, an additional systematic uncertainty of 0.24 GeV is assigned to account for the experimental uncertainty in the Higgs boson mass [48]. The impact of this uncertainty is comparable to the one from PES.

The analysis is limited by the statistical precision. The systematic uncertainties worsen the expected cross section limits by at most 1.5 and 3.8% in the resonant and nonresonant searches, respectively.

Table 5: Summaries of systematic uncertainties. For the normalization uncertainties, the values in the right column indicate the impact on the signal normalization. The uncertainty in the b tagging efficiency is anticorrelated between the b tag categories. The uncertainty in the $m^{\text{kin}}_{\gamma\gamma\text{jj}}$ categorization is anticorrelated between $m^{\text{kin}}_{\gamma\gamma\text{jj}}$ categories for the nonresonant search.

General uncertainties in normalization	
Integrated luminosity	2.6%
Diphoton trigger efficiency	1.0%
Diphoton selection efficiency	1.0%
Resonant low-mass and nonresonant analyses: 2D fit to $m_{\gamma\gamma}$ and m_{jj}	
———————- Uncertainties in normalization ———————-	
Acceptance in p^{j}_{T} (JES and JER)	1.0%
b tagging efficiency in the high-purity category	5.0%
b tagging efficiency in the medium-purity category	
Low-mass resonant and nonresonant $m^{\text{kin}}_{\gamma\gamma\text{jj}} < 350\,\text{GeV}$	2.1%
Nonresonant $m^{\text{kin}}_{\gamma\gamma\text{jj}} > 350\,\text{GeV}$	2.8%
$m^{\text{kin}}_{\gamma\gamma\text{jj}}$ acceptance (PES, JES, PER and JER)	
Low-mass resonant	1.5%
Nonresonant $m^{\text{kin}}_{\gamma\gamma\text{jj}} < 350\,\text{GeV}$ categories	1.5%
Nonresonant $m^{\text{kin}}_{\gamma\gamma\text{jj}} > 350\,\text{GeV}$ categories	0.5%
———————- Uncertainties in the PD parameters ———————-	
m_{jj} resolution (JER), $\frac{\Delta\sigma^{\text{G}}_{\text{jj}}}{\sigma^{\text{G}}_{\text{jj}}}$ and $\frac{\Delta\sigma^{\text{CB}}_{\text{jj}}}{\sigma^{\text{CB}}_{\text{jj}}}$	10%
m_{jj} scale (JES), $\frac{\Delta\mu_{\text{jj}}}{\mu_{\text{jj}}}$	2.6%
$m_{\gamma\gamma}$ resolution (PER), $\frac{\Delta\sigma^{\text{G}}_{\gamma\gamma}}{\sigma^{\text{G}}_{\gamma\gamma}}$ and $\frac{\Delta\sigma^{\text{CB}}_{\gamma\gamma}}{\sigma^{\text{CB}}_{\gamma\gamma}}$	5%
$m_{\gamma\gamma}$ scale (PES and uncertainty in m_{H})	
Low-mass resonant, $\frac{\Delta\mu_{\gamma\gamma}}{\mu_{\gamma\gamma}}$	0.4%
Nonresonant, $\frac{\Delta\mu_{\gamma\gamma}}{\mu_{\gamma\gamma}}$	0.5%
High-mass resonant analysis: 1D fit to $m^{\text{kin}}_{\gamma\gamma\text{jj}}$	
———————- Uncertainties in normalization ———————-	
b tagging efficiency in the high-purity category	5.0%
b tagging efficiency in the medium-purity category	2.8%
m_{jj} and p^{j}_{T} acceptance related to JES and JER	1.5%
$m_{\gamma\gamma}$ selection acceptance related to PES and PER	0.5%
Extra high p^{γ}_{T} normalization uncertainty	5.0%
———————- Uncertainties in the PD parameters ———————-	
$m^{\text{kin}}_{\gamma\gamma\text{jj}}$ scale (PES and JES), $\frac{\Delta\mu^{\text{kin}}_{\gamma\gamma\text{jj}}}{\mu^{\text{kin}}_{\gamma\gamma\text{jj}}}$	1.4%
$m^{\text{kin}}_{\gamma\gamma\text{jj}}$ resolution (PER and JER), $\frac{\Delta\sigma^{\text{G, kin}}_{\gamma\gamma\text{jj}}}{\sigma^{\text{G, kin}}_{\gamma\gamma\text{jj}}}$ and $\frac{\Delta\sigma^{\text{CB, kin}}_{\gamma\gamma\text{jj}}}{\sigma^{\text{CB, kin}}_{\gamma\gamma\text{jj}}}$	10.0%

7 Results

No significant excess is observed over the background expectation in the resonant or nonresonant searches. Upper limits are computed using the modified frequentist approach for confidence levels (CL_s), taking the profile likelihood as a test statistic [76, 77] in the asymptotic approximation. The limits are subsequently compared to theoretical predictions assuming SM branching fractions for Higgs boson decays.

7.1 Resonant signal

The observed and median expected upper limits for all the data at 95% CL are shown in the top of Fig. 9, and at the bottom in a zoomed-in view of the low-mass region. The expected limits range from 1.99 fb for $m_X = 310\,\text{GeV}$ to 0.39 fb for $m_X = 1\,\text{TeV}$. At the transition point between the low-mass and high-mass searches, $m_X = 400\,\text{GeV}$, results with both methods are provided. An improvement of about 20% is observed from the use of the 2D model approach with respect to the 1D analysis.

The result is compared with the cross sections for KK-graviton and radion production in WED models. The tools used to calculate the cross sections for the production of KK graviton in the bulk and RS1 models are described in Refs. [78, 79]. The implementation of the calculations is described in Ref. [80]. In analogy with the Higgs boson, the radion field is predominantly produced through gluon-gluon fusion [81, 82]. The cross section for radion production is calculated at NLO electroweak and next-to-next-to-leading logarithmic QCD accuracy, using the recipe suggested in Ref. [18]. This recipe consists of multiplying the radion cross section based on the fundamental parameter of the theory, Λ_R, by a K-factor calculated for SM-like Higgs boson production through gluon-gluon fusion [36, 83]. The calculations are performed for the SM-like Higgs boson with masses up to 1 TeV. We use the CTEQ6L PDF [84] in these calculations. No mixing between a radion and the Higgs boson is considered in this paper.

In Table 6, we summarize the inclusive production cross sections and the branching fractions of the heavy resonances in the theoretical benchmarks we use for interpretation. The absolute values of the production cross sections scale with $(k/\overline{M}_{Pl})^2$ for the KK Graviton [22] and with $1/\Lambda_R^2$ for the radion [85].

The values for the branching fractions of the resonances in the theory benchmarks do not depend on the fundamental parameters of the theory. The resonance decays have a phase space suppression, related to the mass difference between the resonance and its decay products. In this way, the decay to a Higgs boson pair is not allowed if $m_X < 250\,\text{GeV}$ nor to top quark pairs if $m_X < 350\,\text{GeV}$. In Table 6, we see that the value of the branching fraction changes with the resonance mass from $m_X = 300$ to $m_X = 500\,\text{GeV}$. The exact pattern of this phenomenon is related to the balance between the different phase space suppressions for decays to HH or to $t\bar{t}$, which depends on the model under consideration.

The analysis excludes a radion with masses below 980 GeV for the radion scale $\Lambda_R = 1\,\text{TeV}$. The search has also sensitivity to the presence of a radion with an ultraviolet cutoff $\Lambda_R = 3\,\text{TeV}$ in the region between 200 and 300 GeV.

The difference in total selection efficiency between the spin-0 (radion) and the spin-2 (KK-graviton) models does not exceed 3%. Thus, the same upper limits that are extracted using a radion simulation can be used directly to exclude a KK graviton with masses between 325 and 450 GeV, assuming $k/\overline{M}_{Pl} = 0.2$. The analysis is not yet sensitive to the presence of a KK graviton in the bulk scenario with the same parameters.

Table 6: Cross section and branching fractions for the benchmark theories used in this paper [22, 85]. The branching fractions does not depend on $k/\overline{M}_{\mathrm{Pl}}$, nor on Λ_{R}.

Model	m_{X} (GeV)	$\sigma(\mathrm{gg} \to \mathrm{X})$ (pb)	$\mathcal{B}(\mathrm{X} \to \mathrm{HH})$
RS1 KK graviton	300	2140	0.03%
$(k/\overline{M}_{\mathrm{Pl}} = 0.2)$	500	172	0.24%
	1000	3.1	0.43%
Bulk-RS KK graviton	300	0.65	0.89%
$(k/\overline{M}_{\mathrm{Pl}} = 0.2)$	500	0.11	8.2%
	1000	0.0021	9.8%
Radion	300	20.7	32%
$(\Lambda_{\mathrm{R}} = 1\,\mathrm{TeV})$	500	3.87	25%
	1000	0.46	24%

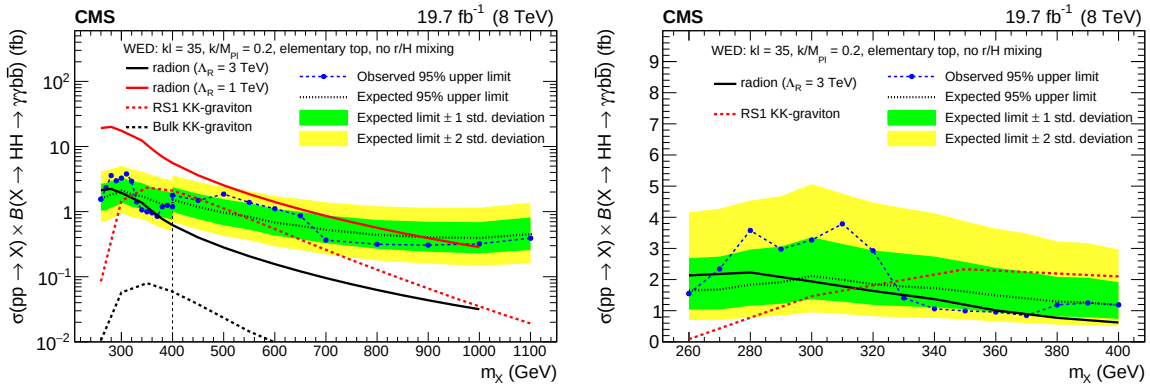

Figure 9: Observed and expected 95% CL upper limits on the product of cross section and the branching fraction $\sigma(\mathrm{pp} \to \mathrm{X})\,\mathcal{B}(\mathrm{X} \to \mathrm{HH} \to \gamma\gamma\mathrm{b\bar{b}})$ obtained through a combination of the two event categories (left), and in the zoomed view at low-mass (right). The green and yellow bands represent, respectively, the 1 and 2 standard deviation extensions beyond the expected limit. Also shown are theoretical predictions corresponding to WED models for radions and RS1 KK gravitons. The upper plot with a logarithmic scale for the y-axis also provides the prediction for the production cross section of a bulk KK graviton. The vertical dashed line in the upper plot shows the separation between the low-mass and high-mass analyses. The limits for $m_{\mathrm{X}} = 400\,\mathrm{GeV}$ are shown for both methods.

7.2 Nonresonant signal

We consider the kinematic properties for new signal identical to those of the SM, but with a different cross section. The observed and expected upper limits on SM-like $gg \to HH \to \gamma\gamma b\bar{b}$ production are, respectively, 1.85 and 1.56 fb. This can be translated into 0.71 and 0.60 pb, respectively, for the total $gg \to HH$ production cross section. The results can also be interpreted in terms of observed and expected limits on the scaling factor $\mu_{HH} < 74$ and $<62^{+37}_{-22}$, respectively. This result provides a quantification of the current analysis relative to the SM prediction.

We also interpret the results in the context of Higgs boson anomalous couplings. The cross section for nonresonant two-Higgs-boson production σ_{HH}^{BSM} in this context can be written as a polynomial in the parameters of the theory relative to the SM nonresonant cross section σ_{HH}^{SM} as:

$$\frac{\sigma_{HH}}{\sigma_{HH}^{SM}} = A_1\,\kappa_t^4 + A_2\,c_2^2 + A_3\,\kappa_t^2\,\kappa_\lambda^2 + (A_6\,c_2 + A_7\,\kappa_t\kappa_\lambda)\kappa_t^2 + A_8\,\kappa_t\kappa_\lambda c_2. \quad (2)$$

The numerical coefficients of Eq. (2) can be calculated by fitting cross sections as described in Ref. [86], obtaining thereby: $A_1 = 2.19$, $A_2 = 9.9$, $A_3 = 0.324$, $A_6 = -8.7$, $A_7 = -1.51$, and $A_8 = 3.0$. Under the assumption that radiative corrections to gluon-gluon fusion of two-Higgs-bosons do not depend significantly on anomalous interactions [87, 88], we normalize σ_{HH} such that, when $\kappa_t = 1$, $\kappa_\lambda = 1$, and $c_2 = 0$, to the cross section that equals the SM prediction at NNLO in QCD.

In Fig. 10, 95% CL limits on nonresonant cross sections are shown, assuming changes only in the trilinear Higgs boson couplings, with the other parameters fixed to their SM values. All κ_λ values are excluded below -17.5 and above 22.5. These results are obtained by extrapolating the limits between the simulated points, as well as above the highest simulated value of κ_λ using Eq. 2, which relies on the similarity of distributions for signal at large values of $|\kappa_\lambda|$ [86, 89], as well as on the behavior of the signal efficiency described in Section 5.4.

Figure 11 shows the 95% CL limits for nonresonant two-Higgs production in the c_2 and κ_t planes for different values of κ_λ. The specific interference pattern for each combination of parameters produces different exclusion limits for different simulated points of parameter space [86, 89]. Only discrete values are provided for limits because a linear interpolation between the simulated points could not follow the strong variations due to interference terms. The points in the theoretical phase space excluded by the data are surrounded by small black boxes. Certain combinations of c_2, κ_λ, or κ_t parameters can be excluded under the assumption that Higgs bosons have their usual SM branching fractions. For example, we observe that $|c_2| \geq 3$ is disfavored by the data when κ_λ and κ_t are fixed to SM values.

8 Summary

A search is performed by the CMS collaboration for resonant and nonresonant production of two Higgs bosons in the decay channel $HH \to \gamma\gamma b\bar{b}$, based on an integrated luminosity of 19.7 fb^{-1} of proton-proton collisions collected at $\sqrt{s} = 8$ TeV. The observations are compatible with expectations from standard model processes. No excess is observed over background predictions.

Resonances are sought in the mass range between 260 and 1100 GeV. Upper limits at a 95% CL are extracted on cross sections for the production of new particles decaying to Higgs boson pairs. The limits are compared to BSM predictions, based on the assumption of the existence of a warped extra dimension. A radion with an ultraviolet cutoff $\Lambda_R = 1$ TeV is excluded with masses below 980 GeV. The search has sensitivity to the presence of a radion with an

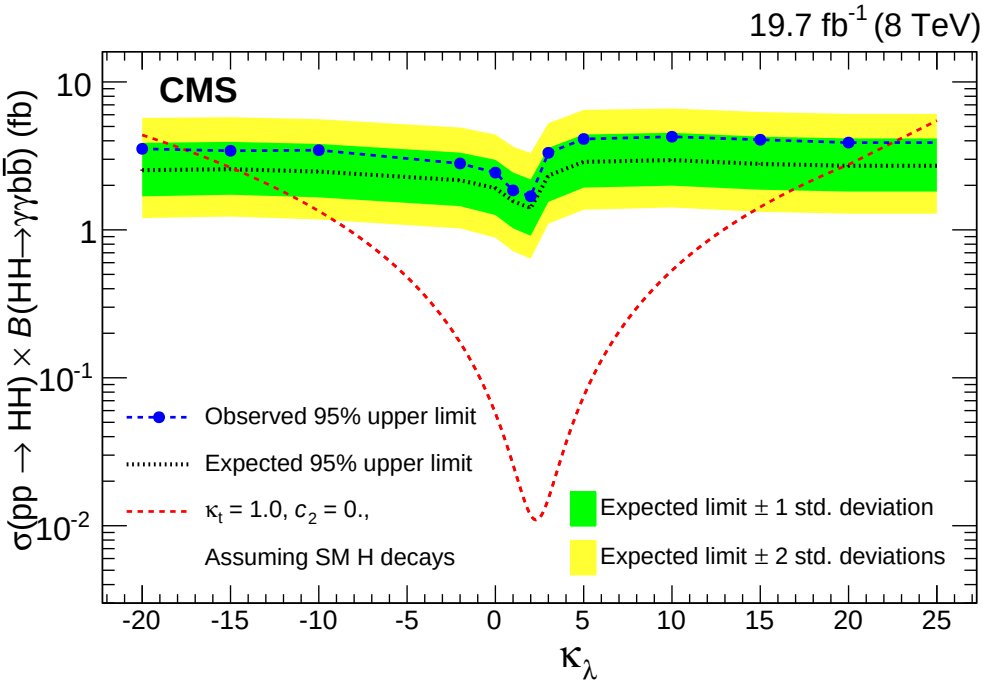

Figure 10: Observed and expected 95% CL upper limits on the product of cross section and the branching fraction $\sigma(\mathrm{pp} \to \mathrm{HH})\,\mathcal{B}(\mathrm{HH} \to \gamma\gamma\mathrm{b\bar{b}})$ for the nonresonant BSM analysis, performed by changing only κ_λ, while keeping all other parameters fixed at the SM predictions.

ultraviolet cutoff $\Lambda_\mathrm{R} = 3\,\mathrm{TeV}$ when its mass lies between 200 and 300 GeV. The RS1 KK graviton is excluded with masses between 325 and 450 GeV for $k/\overline{M}_\mathrm{Pl} = 0.2$. The analysis is not yet sensitive to the presence of a KK graviton in the bulk scenario with the same parameters.

For nonresonant production with SM-like kinematics, a 95% CL upper limit of 1.85 fb is set for the product of the HH cross section and branching fraction, corresponding to a factor 74 larger than the SM value. When only the trilinear Higgs boson coupling is changed, values of the self coupling are excluded for $\kappa_\lambda < -17$ and $\kappa_\lambda > 22.5$. The parameter space is also probed for the presence of other anomalous Higgs boson couplings.

Acknowledgments

We are grateful to B. Hespel, F. Maltoni, E. Vryonidou, and M. Zaro for a customized model of the nonresonant signal generation.

We congratulate our colleagues in the CERN accelerator departments for the excellent performance of the LHC and thank the technical and administrative staffs at CERN and at other CMS institutes for their contributions to the success of the CMS effort. In addition, we gratefully acknowledge the computing centres and personnel of the Worldwide LHC Computing Grid for delivering so effectively the computing infrastructure essential to our analyses. Finally, we acknowledge the enduring support for the construction and operation of the LHC and the CMS detector provided by the following funding agencies: the Austrian Federal Ministry of Science, Research and Economy and the Austrian Science Fund; the Belgian Fonds de la Recherche Scientifique, and Fonds voor Wetenschappelijk Onderzoek; the Brazilian Funding Agencies (CNPq, CAPES, FAPERJ, and FAPESP); the Bulgarian Ministry of Education and Science; CERN; the Chinese Academy of Sciences, Ministry of Science and Technology, and Na-

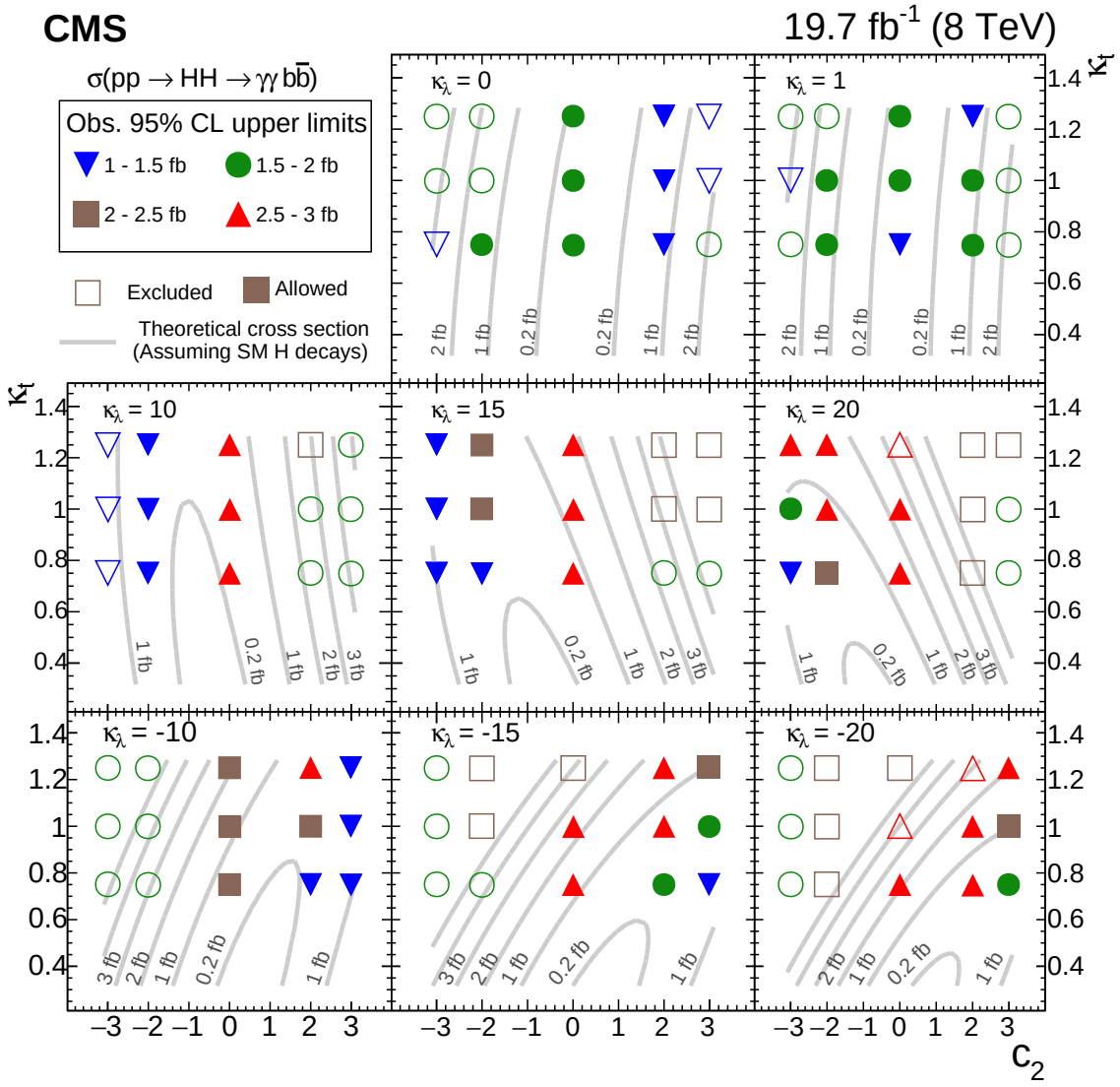

Figure 11: The observed 95% CL limits for nonresonant two-Higgs production in the c_2 and κ_t planes for different values of κ_λ. The different markers symbolize the range in which the upper limits in the cross sections are relevant. The results are compared to the theoretical prediction. The gray lines represent contours of equal cross section, as calculated using Eq. (2). The boxed-in cross section markers provide the combination of parameters excluded at 95% CL.

tional Natural Science Foundation of China; the Colombian Funding Agency (COLCIENCIAS); the Croatian Ministry of Science, Education and Sport, and the Croatian Science Foundation; the Research Promotion Foundation, Cyprus; the Ministry of Education and Research, Estonian Research Council via IUT23-4 and IUT23-6 and European Regional Development Fund, Estonia; the Academy of Finland, Finnish Ministry of Education and Culture, and Helsinki Institute of Physics; the Institut National de Physique Nucléaire et de Physique des Particules / CNRS, and Commissariat à l'Énergie Atomique et aux Énergies Alternatives / CEA, France; the Bundesministerium für Bildung und Forschung, Deutsche Forschungsgemeinschaft, and Helmholtz-Gemeinschaft Deutscher Forschungszentren, Germany; the General Secretariat for Research and Technology, Greece; the National Scientific Research Foundation, and National Innovation Office, Hungary; the Department of Atomic Energy and the Department of Science and Technology, India; the Institute for Studies in Theoretical Physics and Mathe-

matics, Iran; the Science Foundation, Ireland; the Istituto Nazionale di Fisica Nucleare, Italy; the Ministry of Science, ICT and Future Planning, and National Research Foundation (NRF), Republic of Korea; the Lithuanian Academy of Sciences; the Ministry of Education, and University of Malaya (Malaysia); the Mexican Funding Agencies (CINVESTAV, CONACYT, SEP, and UASLP-FAI); the Ministry of Business, Innovation and Employment, New Zealand; the Pakistan Atomic Energy Commission; the Ministry of Science and Higher Education and the National Science Centre, Poland; the Fundação para a Ciência e a Tecnologia, Portugal; JINR, Dubna; the Ministry of Education and Science of the Russian Federation, the Federal Agency of Atomic Energy of the Russian Federation, Russian Academy of Sciences, and the Russian Foundation for Basic Research; the Ministry of Education, Science and Technological Development of Serbia; the Secretaría de Estado de Investigación, Desarrollo e Innovación and Programa Consolider-Ingenio 2010, Spain; the Swiss Funding Agencies (ETH Board, ETH Zurich, PSI, SNF, UniZH, Canton Zurich, and SER); the Ministry of Science and Technology, Taipei; the Thailand Center of Excellence in Physics, the Institute for the Promotion of Teaching Science and Technology of Thailand, Special Task Force for Activating Research and the National Science and Technology Development Agency of Thailand; the Scientific and Technical Research Council of Turkey, and Turkish Atomic Energy Authority; the National Academy of Sciences of Ukraine, and State Fund for Fundamental Researches, Ukraine; the Science and Technology Facilities Council, UK; the US Department of Energy, and the US National Science Foundation.

Individuals have received support from the Marie-Curie programme and the European Research Council and EPLANET (European Union); the Leventis Foundation; the A. P. Sloan Foundation; the Alexander von Humboldt Foundation; the Belgian Federal Science Policy Office; the Fonds pour la Formation à la Recherche dans l'Industrie et dans l'Agriculture (FRIA-Belgium); the Agentschap voor Innovatie door Wetenschap en Technologie (IWT-Belgium); the Ministry of Education, Youth and Sports (MEYS) of the Czech Republic; the Council of Science and Industrial Research, India; the HOMING PLUS programme of the Foundation for Polish Science, cofinanced from European Union, Regional Development Fund; the OPUS programme of the National Science Center (Poland); the Compagnia di San Paolo (Torino); MIUR project 20108T4XTM (Italy); the Thalis and Aristeia programmes cofinanced by EU-ESF and the Greek NSRF; the National Priorities Research Program by Qatar National Research Fund; the Rachadapisek Sompot Fund for Postdoctoral Fellowship, Chulalongkorn University (Thailand); the Chulalongkorn Academic into Its 2nd Century Project Advancement Project (Thailand); and the Welch Foundation, contract C-1845.

References

[1] CMS Collaboration, "Observation of a new boson at a mass of 125 GeV with the CMS experiment at the LHC", *Phys. Lett. B* **716** (2012) 30, doi:10.1016/j.physletb.2012.08.021, arXiv:1207.7235.

[2] ATLAS Collaboration, "Observation of a new particle in the search for the Standard Model Higgs boson with the ATLAS detector at the LHC", *Phys. Lett. B* **716** (2012) 1, doi:10.1016/j.physletb.2012.08.020, arXiv:1207.7214.

[3] D. de Florian and J. Mazzitelli, "Higgs Boson Pair Production at Next-to-Next-to-Leading Order in QCD", *Phys. Rev. Lett.* **111** (2013) 201801, doi:10.1103/PhysRevLett.111.201801, arXiv:1309.6594.

[4] S. Dawson, S. Dittmaier, and M. Spira, "Neutral Higgs boson pair production at hadron colliders: QCD corrections", *Phys. Rev. D* **58** (1998) 115012, doi:10.1103/PhysRevD.58.115012, arXiv:hep-ph/9805244.

[5] J. Baglio et al., "The measurement of the Higgs self-coupling at the LHC: theoretical status", *JHEP* **04** (2013) 151, doi:10.1007/JHEP04(2013)151, arXiv:1212.5581.

[6] S. Dawson, A. Ismail, and I. Low, "What's in the loop? The anatomy of double Higgs production", *Phys. Rev. D* **91** (2015) 115008, doi:10.1103/PhysRevD.91.115008, arXiv:1504.05596.

[7] Z. Heng, L. Shang, Y. Zhang, and J. Zhu, "Pair production of 125 GeV Higgs boson in the SM extension with color-octet scalars at the LHC", *JHEP* **02** (2014) 083, doi:10.1007/JHEP02(2014)083, arXiv:1312.4260.

[8] R. Gröber and M. Mühlleitner, "Composite Higgs boson pair production at the LHC", *JHEP* **06** (2011) 020, doi:10.1007/JHEP06(2011)020, arXiv:1012.1562.

[9] M. Moretti et al., "Higgs boson self-couplings at the LHC as a probe of extended Higgs sectors", *JHEP* **02** (2005) 024, doi:10.1088/1126-6708/2005/02/024, arXiv:hep-ph/0410334.

[10] L. Randall and R. Sundrum, "Large Mass Hierarchy from a Small Extra Dimension", *Phys. Rev. Lett.* **83** (1999) 3370, doi:10.1103/PhysRevLett.83.3370, arXiv:hep-ph/9905221.

[11] W. D. Goldberger and M. B. Wise, "Modulus Stabilization with Bulk Fields", *Phys. Rev. Lett.* **83** (1999) 4922, doi:10.1103/PhysRevLett.83.4922, arXiv:hep-ph/9907447.

[12] O. DeWolfe, D. Z. Freedman, S. S. Gubser, and A. Karch, "Modeling the fifth dimension with scalars and gravity", *Phys. Rev. D* **62** (2000) 046008, doi:10.1103/PhysRevD.62.046008, arXiv:hep-th/9909134.

[13] C. Csáki, M. Graesser, L. Randall, and J. Terning, "Cosmology of brane models with radion stabilization", *Phys. Rev. D* **62** (2000) 045015, doi:10.1103/PhysRevD.62.045015, arXiv:hep-ph/9911406.

[14] H. Davoudiasl, J. L. Hewett, and T. G. Rizzo, "Phenomenology of the Randall–Sundrum Gauge Hierarchy Model", *Phys. Rev. Lett.* **84** (2000) 2080, doi:10.1103/PhysRevLett.84.2080, arXiv:hep-ph/9909255.

[15] C. Csáki, M. L. Graesser, and G. D. Kribs, "Radion dynamics and electroweak physics", *Phys. Rev. D* **63** (2001) 065002, doi:10.1103/PhysRevD.63.065002, arXiv:hep-th/0008151.

[16] K. Agashe, H. Davoudiasl, G. Perez, and A. Soni, "Warped gravitons at the CERN LHC and beyond", *Phys. Rev. D* **76** (2007) 036006, doi:10.1103/PhysRevD.76.036006, arXiv:hep-ph/0701186.

[17] A. L. Fitzpatrick, J. Kaplan, L. Randall, and L.-T. Wang, "Searching for the Kaluza-Klein graviton in bulk RS models", *JHEP* **09** (2007) 013, doi:10.1088/1126-6708/2007/09/013, arXiv:hep-ph/0701150.

[18] G. F. Giudice, R. Rattazzi, and J. D. Wells, "Graviscalars from higher-dimensional metrics and curvature-Higgs mixing", *Nucl. Phys. B* **595** (2001) 250, doi:10.1016/S0550-3213(00)00686-6, arXiv:hep-ph/0002178.

[19] D. Dominici, B. Grzadkowski, J. F. Gunion, and M. Toharia, "The scalar sector of the Randall–Sundrum model", *Nucl. Phys. B* **671** (2003) 243, doi:10.1016/j.nuclphysb.2003.08.020, arXiv:hep-ph/0206192.

[20] I. Antoniadis and R. Sturani, "Higgs graviscalar mixing in type I string theory", *Nucl. Phys. B* **631** (2002) 66, doi:10.1016/S0550-3213(02)00214-6, arXiv:hep-th/0201166.

[21] N. Desai, U. Maitra, and B. Mukhopadhyaya, "An updated analysis of radion-Higgs mixing in the light of LHC data", *JHEP* **10** (2013) 093, doi:10.1007/JHEP10(2013)093, arXiv:1307.3765.

[22] A. Oliveira and R. Rosenfeld, "Graviscalars from higher-dimensional metrics and curvature-Higgs mixing", *Phys. Lett. B* **702** (2011) 201, doi:10.1016/j.physletb.2011.06.086, arXiv:1009.4497.

[23] D. O'Connell, M. J. Ramsey-Musolf, and M. B. Wise, "Minimal extension of the standard model scalar sector", *Phys. Rev. D* **75** (2007) 037701, doi:10.1103/PhysRevD.75.037701, arXiv:hep-ph/0611014.

[24] G. C. Branco et al., "Theory and phenomenology of two-Higgs-doublet modeld", *Phys. Rept.* **516** (2012) 1, doi:10.1016/j.physrep.2012.02.002, arXiv:1106.0034.

[25] A. Djouadi, "The anatomy of electroweak symmetry breaking Tome II: The Higgs bosons in the Minimal Supersymmetric Model", *Phys. Rept.* **459** (2008) 1, doi:10.1016/j.physrep.2007.10.005, arXiv:hep-ph/0503173.

[26] R. Barbieri et al., "One or more Higgs bosons?", *Phys. Rev. D* **88** (2013) 055011, doi:10.1103/PhysRevD.88.055011, arXiv:1307.4937.

[27] H. Georgi and M. Machacek, "Doubly charged Higgs bosons", *Nucl. Phys. B* **262** (1985) 463, doi:10.1016/0550-3213(85)90325-6.

[28] E. W. N. Glover and J. J. van der Bij, "Higgs Boson Pair Production via Gluon Fusion", *Nucl. Phys. B* **309** (1988) 282, doi:10.1016/0550-3213(88)90083-1.

[29] T. Plehn, M. Spira, and P. M. Zerwas, "Pair production of neutral Higgs particles in gluon-gluon collisions", *Nucl. Phys. B* **479** (1996) 46, doi:10.1016/0550-3213(96)00418-X, arXiv:hep-ph/9603205. [Erratum: doi:10.1016/S0550-3213(98)00406-4].

[30] A. Djouadi, W. Kilian, M. Mühlleitner, and P. M. Zerwas, "Production of neutral Higgs boson pairs at LHC", *Eur. Phys. J. C* **10** (1999) 45, doi:10.1007/s100529900083, arXiv:hep-ph/9904287.

[31] U. Baur, T. Plehn, and D. L. Rainwater, "Probing the Higgs self-coupling at hadron colliders using rare decays", *Phys. Rev. D* **69** (2004) 053004, doi:10.1103/PhysRevD.69.053004, arXiv:hep-ph/0310056.

[32] A. Pierce, J. Thaler, and L.-T. Wang, "Disentangling dimension six operators through di-Higgs boson production", *JHEP* **05** (2007) 070, doi:10.1088/1126-6708/2007/05/070, arXiv:hep-ph/0609049.

[33] K. Nishiwaki, S. Niyogi, and A. Shivaji, "$t\bar{t}H$ anomalous coupling in double Higgs production", *JHEP* **04** (2014) 011, doi:10.1007/JHEP04(2014)011, arXiv:1309.6907.

[34] F. Goertz, A. Papaefstathiou, L. L. Yang, and J. Zurita, "Higgs boson pair production in the D=6 extension of the SM", *JHEP* **04** (2015) 167, doi:10.1007/JHEP04(2015)167, arXiv:1410.3471.

[35] N. Liu, S. Hu, B. Yang, and J. Han, "Impact of top-Higgs couplings on Di-Higgs production at future colliders", *JHEP* **01** (2015) 008, doi:10.1007/JHEP01(2015)008, arXiv:1408.4191.

[36] S. Heinemeyer et al., "Handbook of LHC Higgs cross sections: 3. Higgs properties", CERN Report CERN-2013-004, 2013. doi:10.5170/CERN-2013-004, arXiv:1307.1347.

[37] J. C. Collins and D. E. Soper, "Angular distribution of dileptons in high-energy hadron collisions", *Phys. Rev. D* **16** (1977) 2219, doi:10.1103/PhysRevD.16.2219.

[38] ATLAS Collaboration, "Search For Higgs Boson Pair Production in the $\gamma\gamma b\bar{b}$ Final State Using pp Collision Data at $\sqrt{s} = 8$ TeV from the ATLAS Detector", *Phys. Rev. Lett.* **114** (2015) 081802, doi:10.1103/PhysRevLett.114.081802, arXiv:1406.5053.

[39] ATLAS Collaboration, "Search for Higgs boson pair production in the $b\bar{b}b\bar{b}$ final state from pp collisions at $\sqrt{s} = 8$ TeV with the ATLAS detector", *Eur. Phys. J. C* **75** (2015) 412, doi:10.1140/epjc/s10052-015-3628-x, arXiv:1506.00285.

[40] ATLAS Collaboration, "Searches for Higgs boson pair production in the $hh \to b\bar{b}\tau\tau, \gamma\gamma WW^*, \gamma\gamma b\bar{b}, b\bar{b}b\bar{b}$ channels with the ATLAS detector", *Phys. Rev. D* **92** (2015) 092004, doi:10.1103/PhysRevD.92.092004, arXiv:1509.04670.

[41] CMS Collaboration, "Searches for heavy Higgs bosons in two-Higgs-doublet models and for $t \to ch$ decay using multilepton and diphoton final states in pp collisions at 8 TeV", *Phys. Rev. D* **90** (2014) 112013, doi:10.1103/PhysRevD.90.112013, arXiv:1410.2751.

[42] CMS Collaboration, "Search for resonant pair production of Higgs bosons decaying to two bottom quark-antiquark pairs in proton-proton collisions at 8 TeV", *Phys. Lett. B* **749** (2015) 560, doi:10.1016/j.physletb.2015.08.047, arXiv:1503.04114.

[43] CMS Collaboration, "Search for heavy resonances decaying to two Higgs bosons in final states containing four b quarks", *Eur. Phys. J. C* **76** (2016) 371, doi:10.1140/epjc/s10052-016-4206-6, arXiv:1602.08762.

[44] CMS Collaboration, "Searches for a heavy scalar boson H decaying to a pair of 125 GeV Higgs bosons hh or for a heavy pseudoscalar boson A decaying to Zh, in the final states with $h \to \tau\tau$", *Phys. Lett. B* **755** (2016) 217, doi:10.1016/j.physletb.2016.01.056, arXiv:1510.01181.

[45] CMS Collaboration, "The CMS experiment at the CERN LHC", *JINST* **3** (2008) S08004, doi:10.1088/1748-0221/3/08/S08004.

[46] J. Alwall et al., "The automated computation of tree-level and next-to-leading order differential cross sections, and their matching to parton shower simulations", *JHEP* **07** (2014) 079, doi:10.1007/JHEP07(2014)079, arXiv:1405.0301.

[47] T. Sjöstrand, S. Mrenna, and P. Skands, "PYTHIA 6.4 physics and manual", *JHEP* **05** (2006) 026, doi:10.1088/1126-6708/2006/05/026, arXiv:hep-ph/0603175.

[48] ATLAS and CMS Collaborations, "Combined Measurement of the Higgs Boson Mass in pp Collisions at $\sqrt{s} = 7$ and 8 TeV with the ATLAS and CMS Experiments", *Phys. Rev. Lett.* **114** (2015) 191803, doi:10.1103/PhysRevLett.114.191803, arXiv:1503.07589.

[49] CMS Collaboration, "Precise determination of the mass of the Higgs boson and tests of compatibility of its couplings with the standard model predictions using proton collisions at 7 and 8 TeV", *Eur. Phys. J. C* **75** (2015) 212, doi:10.1140/epjc/s10052-015-3351-7, arXiv:1412.8662.

[50] T. Corbett et al., "The Non-Linear Higgs Legacy of the LHC Run I", (2015). arXiv:1511.08188.

[51] T. Gleisberg et al., "Event generation with SHERPA 1.1", *JHEP* **02** (2009) 007, doi:10.1088/1126-6708/2009/02/007, arXiv:0811.4622.

[52] P. Nason, "A new method for combining NLO QCD with shower Monte Carlo algorithms", *JHEP* **11** (2004) 040, doi:10.1088/1126-6708/2004/11/040, arXiv:hep-ph/0409146.

[53] S. Frixione, P. Nason, and C. Oleari, "Matching NLO QCD computations with parton shower simulations: the POWHEG method", *JHEP* **11** (2007) 070, doi:10.1088/1126-6708/2007/11/070, arXiv:0709.2092.

[54] S. Alioli, P. Nason, C. Oleari, and E. Re, "A general framework for implementing NLO calculations in shower Monte Carlo programs: the POWHEG BOX", *JHEP* **06** (2010) 043, doi:10.1007/JHEP06(2010)043, arXiv:1002.2581.

[55] GEANT4 Collaboration, "GEANT4—a simulation toolkit", *Nucl. Instrum. Meth. A* **506** (2003) 250, doi:10.1016/S0168-9002(03)01368-8.

[56] J. Allison et al., "Geant4 developments and applications", *IEEE Trans. Nucl. Sci.* **53** (2006) 270, doi:10.1109/TNS.2006.869826.

[57] CMS Collaboration, "Observation of the diphoton decay of the Higgs boson and measurement of its properties", *Eur. Phys. J. C* **74** (2014) 3076, doi:10.1140/epjc/s10052-014-3076-z, arXiv:1407.0558.

[58] CMS Collaboration, "Photon reconstruction and identification at $\sqrt{s} = 7$ TeV", CMS Physics Analysis Summary CMS-PAS-EGM-10-005, 2010.

[59] CMS Collaboration, "Isolated Photon Reconstruction and Identification at $\sqrt{s} = 7$ TeV", CMS Physics Analysis Summary CMS-PAS-EGM-10-006, 2011.

[60] CMS Collaboration, "Energy calibration and resolution of the CMS electromagnetic calorimeter in pp Collisions at $\sqrt{s} = 7$ TeV", *JINST* **8** (2013) P09009, doi:10.1088/1748-0221/8/09/P09009, arXiv:1306.2016.

[61] CMS Collaboration, "Search for the standard model Higgs boson produced in association with a W or a Z boson and decaying to bottom quarks", *Phys. Rev. D* **89** (2014) 012003, doi:10.1103/PhysRevD.89.012003, arXiv:1310.3687.

[62] CMS Collaboration, "Particle–Flow Event Reconstruction in CMS and Performance for Jets, Taus, and $E_{\mathrm{T}}^{\mathrm{miss}}$", CMS Physics Analysis Summary CMS-PAS-PFT-09-001, 2009.

[63] CMS Collaboration, "Commissioning of the Particle–Flow Event Reconstruction with the first LHC collisions recorded in the CMS detector", CMS Physics Analysis Summary CMS-PAS-PFT-10-001, 2010.

[64] M. Cacciari, G. P. Salam, and G. Soyez, "The anti-k_t jet clustering algorithm", *JHEP* **04** (2008) 063, doi:10.1088/1126-6708/2008/04/063, arXiv:0802.1189.

[65] M. Cacciari and G. P. Salam, "Pileup subtraction using jet areas", *Phys. Lett. B* **659** (2008) 119, doi:10.1016/j.physletb.2007.09.077, arXiv:0707.1378.

[66] M. Cacciari, G. P. Salam, and G. Soyez, "FastJet User Manual", *Eur. Phys. J. C* **72** (2012) 1896, doi:10.1140/epjc/s10052-012-1896-2, arXiv:1111.6097.

[67] CMS Collaboration, "Determination of jet energy calibration and transverse momentum resolution in CMS", *JINST* **6** (2011) P11002, doi:10.1088/1748-0221/6/11/P11002, arXiv:1107.4277.

[68] CMS Collaboration, "Status of the 8 TeV Jet Energy Corrections and Uncertainties based on 11 fb^{-1} of Data in CMS", technical report, 2013.

[69] CMS Collaboration, "Identification of b-quark jets with the CMS experiment", *JINST* **8** (2013) P04013, doi:10.1088/1748-0221/8/04/P04013, arXiv:1211.4462.

[70] CMS Collaboration, "Search for a standard-model-like Higgs boson with a mass in the range 145 to 1000 GeV at the LHC", *Eur. Phys. J. C* **73** (2013) 2469, doi:10.1140/epjc/s10052-013-2469-8, arXiv:1304.0213.

[71] CMS Collaboration, "Search for a fermiophobic Higgs boson in pp collisions at $\sqrt{s} = 7$ TeV", *JHEP* **09** (2012) 111, doi:10.1007/JHEP09(2012)111, arXiv:1207.1130.

[72] M. J. Oreglia, "A study of the reactions $\psi' \to \gamma\gamma\psi$". PhD thesis, Stanford University, 1980. SLAC Report SLAC-R-236.

[73] M. Gouzevitch et al., "Scale-invariant resonance tagging in multijet events and new physics in Higgs pair production", *JHEP* **07** (2013) 148, doi:10.1007/JHEP07(2013)148, arXiv:1303.6636.

[74] CMS Collaboration, "CMS Luminosity Based on Pixel Cluster Counting - Summer 2013 Update", CMS Physics Analysis Summary CMS-PAS-LUM-13-001, 2013.

[75] LHC Higgs Cross Section Working Group, S. Dittmaier et al., "Handbook of LHC Higgs Cross Sections: 1. Inclusive Observables", CERN Report CERN-2011-002, 2011. doi:10.5170/CERN-2011-002, arXiv:1101.0593.

[76] A. L. Read, "Presentation of search results: the CL_s technique", *J. Phys. G* **28** (2002) 2693, doi:10.1088/0954-3899/28/10/313.

[77] T. Junk, "Confidence level computation for combining searches with small statistics", *Nucl. Instrum. Meth. A* **434** (1999) 435, doi:10.1016/S0168-9002(99)00498-2, arXiv:hep-ex/9902006.

[78] K. Agashe et al., "Warped Extra Dimensional Benchmarks for Snowmass 2013", in *Community Summer Study 2013: Snowmass on the Mississippi (CSS2013) Minneapolis, MN, USA, July 29-August 6, 2013*. 2013. arXiv:1309.7847.

[79] P. de Aquino, K. Hagiwara, Q. Li, and F. Maltoni, "Simulating graviton production at hadron colliders", *JHEP* **06** (2011) 132, doi:10.1007/JHEP06(2011)132, arXiv:1101.5499.

[80] A. Oliveira, "Gravity particles from Warped Extra Dimensions, a review. Part I - KK Graviton", (2014). arXiv:1404.0102.

[81] U. Mahanta and A. Datta, "Search prospects of light stabilized radions at Tevatron and LHC", *Phys. Lett. B* **483** (2000) 196, doi:10.1016/S0370-2693(00)00560-8, arXiv:hep-ph/0002183.

[82] H. Davoudiasl, J. L. Hewett, and T. G. Rizzo, "Experimental probes of localized gravity: On and off the wall", *Phys. Rev. D* **63** (2001) 075004, doi:10.1103/PhysRevD.63.075004, arXiv:hep-ph/0006041.

[83] S. Catani, D. de Florian, M. Grazzini, and P. Nason, "Soft gluon resummation for Higgs boson production at hadron colliders", *JHEP* **07** (2003) 028, doi:10.1088/1126-6708/2003/07/028, arXiv:hep-ph/0306211.

[84] P. M. Nadolsky et al., "Implications of CTEQ global analysis for collider observables", *Phys. Rev. D* **78** (2008) 013004, doi:10.1103/PhysRevD.78.013004, arXiv:0802.0007.

[85] V. Barger and M. Ishida, "Randall–Sundrum reality at the LHC", *Phys. Lett. B* **709** (2012) 185, doi:10.1016/j.physletb.2012.01.073, arXiv:1110.6452.

[86] A. Carvalho et al., "Higgs Pair Production: Choosing Benchmarks With Cluster Analysis", *JHEP* **04** (2016) 126, doi:10.1007/JHEP04(2016)126, arXiv:1507.02245.

[87] R. Gröber, M. Mühlleitner, M. Spira, and J. Streicher, "NLO QCD corrections to Higgs pair production including dimension-6 operators", *JHEP* **09** (2015) 092, doi:10.1007/JHEP09(2015)092, arXiv:1504.06577.

[88] D. de Florian and J. Mazzitelli, "Higgs pair production at next-to-next-to-leading logarithmic accuracy at the LHC", *JHEP* **09** (2015) 053, doi:10.1007/JHEP09(2015)053, arXiv:1505.7122.

[89] A. Carvalho et al., "Analytical parametrization and shape classification of anomalous HH production in the EFT approach", (2016). arXiv:1608.06578.

A The CMS Collaboration

Yerevan Physics Institute, Yerevan, Armenia
V. Khachatryan, A.M. Sirunyan, A. Tumasyan

Institut für Hochenergiephysik der OeAW, Wien, Austria
W. Adam, E. Asilar, T. Bergauer, J. Brandstetter, E. Brondolin, M. Dragicevic, J. Erö, M. Flechl, M. Friedl, R. Frühwirth[1], V.M. Ghete, C. Hartl, N. Hörmann, J. Hrubec, M. Jeitler[1], A. König, M. Krammer[1], I. Krätschmer, D. Liko, T. Matsushita, I. Mikulec, D. Rabady, N. Rad, B. Rahbaran, H. Rohringer, J. Schieck[1], J. Strauss, W. Treberer-Treberspurg, W. Waltenberger, C.-E. Wulz[1]

National Centre for Particle and High Energy Physics, Minsk, Belarus
V. Mossolov, N. Shumeiko, J. Suarez Gonzalez

Universiteit Antwerpen, Antwerpen, Belgium
S. Alderweireldt, T. Cornelis, E.A. De Wolf, X. Janssen, A. Knutsson, J. Lauwers, S. Luyckx, M. Van De Klundert, H. Van Haevermaet, P. Van Mechelen, N. Van Remortel, A. Van Spilbeeck

Vrije Universiteit Brussel, Brussel, Belgium
S. Abu Zeid, F. Blekman, J. D'Hondt, N. Daci, I. De Bruyn, K. Deroover, N. Heracleous, J. Keaveney, S. Lowette, S. Moortgat, L. Moreels, A. Olbrechts, Q. Python, D. Strom, S. Tavernier, W. Van Doninck, P. Van Mulders, I. Van Parijs

Université Libre de Bruxelles, Bruxelles, Belgium
H. Brun, C. Caillol, B. Clerbaux, G. De Lentdecker, G. Fasanella, L. Favart, R. Goldouzian, A. Grebenyuk, G. Karapostoli, T. Lenzi, A. Léonard, T. Maerschalk, A. Marinov, A. Randleconde, T. Seva, C. Vander Velde, P. Vanlaer, R. Yonamine, F. Zenoni, F. Zhang[2]

Ghent University, Ghent, Belgium
L. Benucci, A. Cimmino, S. Crucy, D. Dobur, A. Fagot, G. Garcia, M. Gul, J. Mccartin, A.A. Ocampo Rios, D. Poyraz, D. Ryckbosch, S. Salva, R. Schöfbeck, M. Sigamani, M. Tytgat, W. Van Driessche, E. Yazgan, N. Zaganidis

Université Catholique de Louvain, Louvain-la-Neuve, Belgium
C. Beluffi[3], O. Bondu, S. Brochet, G. Bruno, A. Caudron, L. Ceard, S. De Visscher, C. Delaere, M. Delcourt, L. Forthomme, B. Francois, A. Giammanco, A. Jafari, P. Jez, M. Komm, V. Lemaitre, A. Magitteri, A. Mertens, M. Musich, C. Nuttens, K. Piotrzkowski, L. Quertenmont, M. Selvaggi, M. Vidal Marono, S. Wertz

Université de Mons, Mons, Belgium
N. Beliy, G.H. Hammad

Centro Brasileiro de Pesquisas Fisicas, Rio de Janeiro, Brazil
W.L. Aldá Júnior, F.L. Alves, G.A. Alves, L. Brito, M. Correa Martins Junior, M. Hamer, C. Hensel, A. Moraes, M.E. Pol, P. Rebello Teles

Universidade do Estado do Rio de Janeiro, Rio de Janeiro, Brazil
E. Belchior Batista Das Chagas, W. Carvalho, J. Chinellato[4], A. Custódio, E.M. Da Costa, D. De Jesus Damiao, C. De Oliveira Martins, S. Fonseca De Souza, L.M. Huertas Guativa, H. Malbouisson, D. Matos Figueiredo, C. Mora Herrera, L. Mundim, H. Nogima, W.L. Prado Da Silva, A. Santoro, A. Sznajder, E.J. Tonelli Manganote[4], A. Vilela Pereira

Universidade Estadual Paulista [a], Universidade Federal do ABC [b], São Paulo, Brazil
S. Ahuja[a], C.A. Bernardes[b], A. De Souza Santos[b], S. Dogra[a], T.R. Fernandez Perez Tomei[a],

E.M. Gregores[b], P.G. Mercadante[b], C.S. Moon[a,5], S.F. Novaes[a], Sandra S. Padula[a], D. Romero Abad[b], J.C. Ruiz Vargas

Institute for Nuclear Research and Nuclear Energy, Sofia, Bulgaria
A. Aleksandrov, R. Hadjiiska, P. Iaydjiev, M. Rodozov, S. Stoykova, G. Sultanov, M. Vutova

University of Sofia, Sofia, Bulgaria
A. Dimitrov, I. Glushkov, L. Litov, B. Pavlov, P. Petkov

Beihang University, Beijing, China
W. Fang[6]

Institute of High Energy Physics, Beijing, China
M. Ahmad, J.G. Bian, G.M. Chen, H.S. Chen, M. Chen, T. Cheng, R. Du, C.H. Jiang, D. Leggat, R. Plestina[7], F. Romeo, S.M. Shaheen, A. Spiezia, J. Tao, C. Wang, Z. Wang, H. Zhang

State Key Laboratory of Nuclear Physics and Technology, Peking University, Beijing, China
C. Asawatangtrakuldee, Y. Ban, Q. Li, S. Liu, Y. Mao, S.J. Qian, D. Wang, Z. Xu

Universidad de Los Andes, Bogota, Colombia
C. Avila, A. Cabrera, L.F. Chaparro Sierra, C. Florez, J.P. Gomez, B. Gomez Moreno, J.C. Sanabria

University of Split, Faculty of Electrical Engineering, Mechanical Engineering and Naval Architecture, Split, Croatia
N. Godinovic, D. Lelas, I. Puljak, P.M. Ribeiro Cipriano

University of Split, Faculty of Science, Split, Croatia
Z. Antunovic, M. Kovac

Institute Rudjer Boskovic, Zagreb, Croatia
V. Brigljevic, D. Ferencek, K. Kadija, J. Luetic, S. Micanovic, L. Sudic

University of Cyprus, Nicosia, Cyprus
A. Attikis, G. Mavromanolakis, J. Mousa, C. Nicolaou, F. Ptochos, P.A. Razis, H. Rykaczewski

Charles University, Prague, Czech Republic
M. Finger[8], M. Finger Jr.[8]

Universidad San Francisco de Quito, Quito, Ecuador
E. Carrera Jarrin

Academy of Scientific Research and Technology of the Arab Republic of Egypt, Egyptian Network of High Energy Physics, Cairo, Egypt
A. Awad, S. Elgammal[9], A. Mohamed[10], E. Salama[9,11]

National Institute of Chemical Physics and Biophysics, Tallinn, Estonia
B. Calpas, M. Kadastik, M. Murumaa, L. Perrini, M. Raidal, A. Tiko, C. Veelken

Department of Physics, University of Helsinki, Helsinki, Finland
P. Eerola, J. Pekkanen, M. Voutilainen

Helsinki Institute of Physics, Helsinki, Finland
J. Härkönen, V. Karimäki, R. Kinnunen, T. Lampén, K. Lassila-Perini, S. Lehti, T. Lindén, P. Luukka, T. Peltola, J. Tuominiemi, E. Tuovinen, L. Wendland

Lappeenranta University of Technology, Lappeenranta, Finland
J. Talvitie, T. Tuuva

DSM/IRFU, CEA/Saclay, Gif-sur-Yvette, France
M. Besancon, F. Couderc, M. Dejardin, D. Denegri, B. Fabbro, J.L. Faure, C. Favaro, F. Ferri, S. Ganjour, A. Givernaud, P. Gras, G. Hamel de Monchenault, P. Jarry, E. Locci, M. Machet, J. Malcles, J. Rander, A. Rosowsky, M. Titov, A. Zghiche

Laboratoire Leprince-Ringuet, Ecole Polytechnique, IN2P3-CNRS, Palaiseau, France
A. Abdulsalam, I. Antropov, S. Baffioni, F. Beaudette, P. Busson, L. Cadamuro, E. Chapon, C. Charlot, O. Davignon, L. Dobrzynski, R. Granier de Cassagnac, M. Jo, S. Lisniak, P. Miné, I.N. Naranjo, M. Nguyen, C. Ochando, G. Ortona, P. Paganini, P. Pigard, S. Regnard, R. Salerno, Y. Sirois, T. Strebler, Y. Yilmaz, A. Zabi

Institut Pluridisciplinaire Hubert Curien, Université de Strasbourg, Université de Haute Alsace Mulhouse, CNRS/IN2P3, Strasbourg, France
J.-L. Agram[12], J. Andrea, A. Aubin, D. Bloch, J.-M. Brom, M. Buttignol, E.C. Chabert, N. Chanon, C. Collard, E. Conte[12], X. Coubez, J.-C. Fontaine[12], D. Gelé, U. Goerlach, C. Goetzmann, A.-C. Le Bihan, J.A. Merlin[13], K. Skovpen, P. Van Hove

Centre de Calcul de l'Institut National de Physique Nucleaire et de Physique des Particules, CNRS/IN2P3, Villeurbanne, France
S. Gadrat

Université de Lyon, Université Claude Bernard Lyon 1, CNRS-IN2P3, Institut de Physique Nucléaire de Lyon, Villeurbanne, France
S. Beauceron, C. Bernet, G. Boudoul, E. Bouvier, C.A. Carrillo Montoya, R. Chierici, D. Contardo, B. Courbon, P. Depasse, H. El Mamouni, J. Fan, J. Fay, S. Gascon, M. Gouzevitch, B. Ille, F. Lagarde, I.B. Laktineh, M. Lethuillier, L. Mirabito, A.L. Pequegnot, S. Perries, A. Popov[14], J.D. Ruiz Alvarez, D. Sabes, V. Sordini, M. Vander Donckt, P. Verdier, S. Viret

Georgian Technical University, Tbilisi, Georgia
T. Toriashvili[15]

Tbilisi State University, Tbilisi, Georgia
Z. Tsamalaidze[8]

RWTH Aachen University, I. Physikalisches Institut, Aachen, Germany
C. Autermann, S. Beranek, L. Feld, A. Heister, M.K. Kiesel, K. Klein, M. Lipinski, A. Ostapchuk, M. Preuten, F. Raupach, S. Schael, C. Schomakers, J.F. Schulte, J. Schulz, T. Verlage, H. Weber, V. Zhukov[14]

RWTH Aachen University, III. Physikalisches Institut A, Aachen, Germany
M. Ata, M. Brodski, E. Dietz-Laursonn, D. Duchardt, M. Endres, M. Erdmann, S. Erdweg, T. Esch, R. Fischer, A. Güth, T. Hebbeker, C. Heidemann, K. Hoepfner, S. Knutzen, M. Merschmeyer, A. Meyer, P. Millet, S. Mukherjee, M. Olschewski, K. Padeken, P. Papacz, T. Pook, M. Radziej, H. Reithler, M. Rieger, F. Scheuch, L. Sonnenschein, D. Teyssier, S. Thüer

RWTH Aachen University, III. Physikalisches Institut B, Aachen, Germany
V. Cherepanov, Y. Erdogan, G. Flügge, H. Geenen, M. Geisler, F. Hoehle, B. Kargoll, T. Kress, A. Künsken, J. Lingemann, A. Nehrkorn, A. Nowack, I.M. Nugent, C. Pistone, O. Pooth, A. Stahl[13]

Deutsches Elektronen-Synchrotron, Hamburg, Germany
M. Aldaya Martin, I. Asin, K. Beernaert, O. Behnke, U. Behrens, K. Borras[16], A. Campbell, P. Connor, C. Contreras-Campana, F. Costanza, C. Diez Pardos, G. Dolinska, S. Dooling, G. Eckerlin, D. Eckstein, T. Eichhorn, E. Gallo[17], J. Garay Garcia, A. Geiser, A. Gizhko,

J.M. Grados Luyando, P. Gunnellini, A. Harb, J. Hauk, M. Hempel[18], H. Jung, A. Kalogeropoulos, O. Karacheban[18], M. Kasemann, J. Kieseler, C. Kleinwort, I. Korol, W. Lange, A. Lelek, J. Leonard, K. Lipka, A. Lobanov, W. Lohmann[18], R. Mankel, I.-A. Melzer-Pellmann, A.B. Meyer, G. Mittag, J. Mnich, A. Mussgiller, E. Ntomari, D. Pitzl, R. Placakyte, A. Raspereza, B. Roland, M.Ö. Sahin, P. Saxena, T. Schoerner-Sadenius, C. Seitz, S. Spannagel, N. Stefaniuk, K.D. Trippkewitz, G.P. Van Onsem, R. Walsh, C. Wissing

University of Hamburg, Hamburg, Germany
V. Blobel, M. Centis Vignali, A.R. Draeger, T. Dreyer, J. Erfle, E. Garutti, K. Goebel, D. Gonzalez, M. Görner, J. Haller, M. Hoffmann, R.S. Höing, A. Junkes, R. Klanner, R. Kogler, N. Kovalchuk, T. Lapsien, T. Lenz, I. Marchesini, D. Marconi, M. Meyer, M. Niedziela, D. Nowatschin, J. Ott, F. Pantaleo[13], T. Peiffer, A. Perieanu, N. Pietsch, J. Poehlsen, C. Sander, C. Scharf, P. Schleper, E. Schlieckau, A. Schmidt, S. Schumann, J. Schwandt, H. Stadie, G. Steinbrück, F.M. Stober, H. Tholen, D. Troendle, E. Usai, L. Vanelderen, A. Vanhoefer, B. Vormwald

Institut für Experimentelle Kernphysik, Karlsruhe, Germany
C. Barth, C. Baus, J. Berger, C. Böser, E. Butz, T. Chwalek, F. Colombo, W. De Boer, A. Descroix, A. Dierlamm, S. Fink, F. Frensch, R. Friese, M. Giffels, A. Gilbert, D. Haitz, F. Hartmann[13], S.M. Heindl, U. Husemann, I. Katkov[14], A. Kornmayer[13], P. Lobelle Pardo, B. Maier, H. Mildner, M.U. Mozer, T. Müller, Th. Müller, M. Plagge, G. Quast, K. Rabbertz, S. Röcker, F. Roscher, M. Schröder, G. Sieber, H.J. Simonis, R. Ulrich, J. Wagner-Kuhr, S. Wayand, M. Weber, T. Weiler, S. Williamson, C. Wöhrmann, R. Wolf

Institute of Nuclear and Particle Physics (INPP), NCSR Demokritos, Aghia Paraskevi, Greece
G. Anagnostou, G. Daskalakis, T. Geralis, V.A. Giakoumopoulou, A. Kyriakis, D. Loukas, A. Psallidas, I. Topsis-Giotis

National and Kapodistrian University of Athens, Athens, Greece
A. Agapitos, S. Kesisoglou, A. Panagiotou, N. Saoulidou, E. Tziaferi

University of Ioánnina, Ioánnina, Greece
I. Evangelou, G. Flouris, C. Foudas, P. Kokkas, N. Loukas, N. Manthos, I. Papadopoulos, E. Paradas, J. Strologas

MTA-ELTE Lendület CMS Particle and Nuclear Physics Group, Eötvös Loránd University
N. Filipovic

Wigner Research Centre for Physics, Budapest, Hungary
G. Bencze, C. Hajdu, P. Hidas, D. Horvath[19], F. Sikler, V. Veszpremi, G. Vesztergombi[20], A.J. Zsigmond

Institute of Nuclear Research ATOMKI, Debrecen, Hungary
N. Beni, S. Czellar, J. Karancsi[21], J. Molnar, Z. Szillasi

University of Debrecen, Debrecen, Hungary
M. Bartók[20], A. Makovec, P. Raics, Z.L. Trocsanyi, B. Ujvari

National Institute of Science Education and Research, Bhubaneswar, India
S. Choudhury[22], P. Mal, K. Mandal, A. Nayak, D.K. Sahoo, N. Sahoo, S.K. Swain

Panjab University, Chandigarh, India
S. Bansal, S.B. Beri, V. Bhatnagar, R. Chawla, R. Gupta, U.Bhawandeep, A.K. Kalsi, A. Kaur, M. Kaur, R. Kumar, A. Mehta, M. Mittal, J.B. Singh, G. Walia

University of Delhi, Delhi, India
Ashok Kumar, A. Bhardwaj, B.C. Choudhary, R.B. Garg, S. Keshri, A. Kumar, S. Malhotra, M. Naimuddin, N. Nishu, K. Ranjan, R. Sharma, V. Sharma

Saha Institute of Nuclear Physics, Kolkata, India
R. Bhattacharya, S. Bhattacharya, K. Chatterjee, S. Dey, S. Dutta, S. Ghosh, N. Majumdar, A. Modak, K. Mondal, S. Mukhopadhyay, S. Nandan, A. Purohit, A. Roy, D. Roy, S. Roy Chowdhury, S. Sarkar, M. Sharan

Bhabha Atomic Research Centre, Mumbai, India
R. Chudasama, D. Dutta, V. Jha, V. Kumar, A.K. Mohanty[13], L.M. Pant, P. Shukla, A. Topkar

Tata Institute of Fundamental Research, Mumbai, India
T. Aziz, S. Banerjee, S. Bhowmik[23], R.M. Chatterjee, R.K. Dewanjee, S. Dugad, S. Ganguly, S. Ghosh, M. Guchait, A. Gurtu[24], Sa. Jain, G. Kole, S. Kumar, B. Mahakud, M. Maity[23], G. Majumder, K. Mazumdar, S. Mitra, G.B. Mohanty, B. Parida, T. Sarkar[23], N. Sur, B. Sutar, N. Wickramage[25]

Indian Institute of Science Education and Research (IISER), Pune, India
S. Chauhan, S. Dube, A. Kapoor, K. Kothekar, A. Rane, S. Sharma

Institute for Research in Fundamental Sciences (IPM), Tehran, Iran
H. Bakhshiansohi, H. Behnamian, S.M. Etesami[26], A. Fahim[27], M. Khakzad, M. Mohammadi Najafabadi, M. Naseri, S. Paktinat Mehdiabadi, F. Rezaei Hosseinabadi, B. Safarzadeh[28], M. Zeinali

University College Dublin, Dublin, Ireland
M. Felcini, M. Grunewald

INFN Sezione di Bari [a], Università di Bari [b], Politecnico di Bari [c], Bari, Italy
M. Abbrescia[a,b], C. Calabria[a,b], C. Caputo[a,b], A. Colaleo[a], D. Creanza[a,c], L. Cristella[a,b], N. De Filippis[a,c], M. De Palma[a,b], L. Fiore[a], G. Iaselli[a,c], G. Maggi[a,c], M. Maggi[a], G. Miniello[a,b], S. My[a,b], S. Nuzzo[a,b], A. Pompili[a,b], G. Pugliese[a,c], R. Radogna[a,b], A. Ranieri[a], G. Selvaggi[a,b], L. Silvestris[a,13], R. Venditti[a,b]

INFN Sezione di Bologna [a], Università di Bologna [b], Bologna, Italy
G. Abbiendi[a], C. Battilana, D. Bonacorsi[a,b], S. Braibant-Giacomelli[a,b], L. Brigliadori[a,b], R. Campanini[a,b], P. Capiluppi[a,b], A. Castro[a,b], F.R. Cavallo[a], S.S. Chhibra[a,b], G. Codispoti[a,b], M. Cuffiani[a,b], G.M. Dallavalle[a], F. Fabbri[a], A. Fanfani[a,b], D. Fasanella[a,b], P. Giacomelli[a], C. Grandi[a], L. Guiducci[a,b], S. Marcellini[a], G. Masetti[a], A. Montanari[a], F.L. Navarria[a,b], A. Perrotta[a], A.M. Rossi[a,b], T. Rovelli[a,b], G.P. Siroli[a,b], N. Tosi[a,b,13]

INFN Sezione di Catania [a], Università di Catania [b], Catania, Italy
G. Cappello[b], M. Chiorboli[a,b], S. Costa[a,b], A. Di Mattia[a], F. Giordano[a,b], R. Potenza[a,b], A. Tricomi[a,b], C. Tuve[a,b]

INFN Sezione di Firenze [a], Università di Firenze [b], Firenze, Italy
G. Barbagli[a], V. Ciulli[a,b], C. Civinini[a], R. D'Alessandro[a,b], E. Focardi[a,b], V. Gori[a,b], P. Lenzi[a,b], M. Meschini[a], S. Paoletti[a], G. Sguazzoni[a], L. Viliani[a,b,13]

INFN Laboratori Nazionali di Frascati, Frascati, Italy
L. Benussi, S. Bianco, F. Fabbri, D. Piccolo, F. Primavera[13]

INFN Sezione di Genova [a], Università di Genova [b], Genova, Italy
V. Calvelli[a,b], F. Ferro[a], M. Lo Vetere[a,b], M.R. Monge[a,b], E. Robutti[a], S. Tosi[a,b]

INFN Sezione di Milano-Bicocca [a], Università di Milano-Bicocca [b], Milano, Italy
L. Brianza, M.E. Dinardo[a,b], S. Fiorendi[a,b], S. Gennai[a], A. Ghezzi[a,b], P. Govoni[a,b], S. Malvezzi[a], R.A. Manzoni[a,b,13], B. Marzocchi[a,b], D. Menasce[a], L. Moroni[a], M. Paganoni[a,b], D. Pedrini[a], S. Pigazzini, S. Ragazzi[a,b], N. Redaelli[a], T. Tabarelli de Fatis[a,b]

INFN Sezione di Napoli [a], Università di Napoli 'Federico II' [b], Napoli, Italy, Università della Basilicata [c], Potenza, Italy, Università G. Marconi [d], Roma, Italy
S. Buontempo[a], N. Cavallo[a,c], S. Di Guida[a,d,13], M. Esposito[a,b], F. Fabozzi[a,c], A.O.M. Iorio[a,b], G. Lanza[a], L. Lista[a], S. Meola[a,d,13], M. Merola[a], P. Paolucci[a,13], C. Sciacca[a,b], F. Thyssen

INFN Sezione di Padova [a], Università di Padova [b], Padova, Italy, Università di Trento [c], Trento, Italy
P. Azzi[a,13], N. Bacchetta[a], M. Bellato[a], L. Benato[a,b], D. Bisello[a,b], A. Boletti[a,b], A. Branca[a,b], R. Carlin[a,b], A. Carvalho Antunes De Oliveira[a,b], P. Checchia[a], M. Dall'Osso[a,b], P. De Castro Manzano[a], T. Dorigo[a], U. Dosselli[a], F. Gasparini[a,b], U. Gasparini[a,b], A. Gozzelino[a], S. Lacaprara[a], M. Margoni[a,b], A.T. Meneguzzo[a,b], J. Pazzini[a,b,13], N. Pozzobon[a,b], P. Ronchese[a,b], F. Simonetto[a,b], E. Torassa[a], M. Tosi[a,b], M. Zanetti, P. Zotto[a,b], A. Zucchetta[a,b], G. Zumerle[a,b]

INFN Sezione di Pavia [a], Università di Pavia [b], Pavia, Italy
A. Braghieri[a], A. Magnani[a,b], P. Montagna[a,b], S.P. Ratti[a,b], V. Re[a], C. Riccardi[a,b], P. Salvini[a], I. Vai[a,b], P. Vitulo[a,b]

INFN Sezione di Perugia [a], Università di Perugia [b], Perugia, Italy
L. Alunni Solestizi[a,b], G.M. Bilei[a], D. Ciangottini[a,b], L. Fanò[a,b], P. Lariccia[a,b], R. Leonardi[a,b], G. Mantovani[a,b], M. Menichelli[a], A. Saha[a], A. Santocchia[a,b]

INFN Sezione di Pisa [a], Università di Pisa [b], Scuola Normale Superiore di Pisa [c], Pisa, Italy
K. Androsov[a,29], P. Azzurri[a,13], G. Bagliesi[a], J. Bernardini[a], T. Boccali[a], R. Castaldi[a], M.A. Ciocci[a,29], R. Dell'Orso[a], S. Donato[a,c], G. Fedi, A. Giassi[a], M.T. Grippo[a,29], F. Ligabue[a,c], T. Lomtadze[a], L. Martini[a,b], A. Messineo[a,b], F. Palla[a], A. Rizzi[a,b], A. Savoy-Navarro[a,30], P. Spagnolo[a], R. Tenchini[a], G. Tonelli[a,b], A. Venturi[a], P.G. Verdini[a]

INFN Sezione di Roma [a], Università di Roma [b], Roma, Italy
L. Barone[a,b], F. Cavallari[a], G. D'imperio[a,b,13], D. Del Re[a,b,13], M. Diemoz[a], S. Gelli[a,b], C. Jorda[a], E. Longo[a,b], F. Margaroli[a,b], P. Meridiani[a], G. Organtini[a,b], R. Paramatti[a], F. Preiato[a,b], S. Rahatlou[a,b], C. Rovelli[a], F. Santanastasio[a,b]

INFN Sezione di Torino [a], Università di Torino [b], Torino, Italy, Università del Piemonte Orientale [c], Novara, Italy
N. Amapane[a,b], R. Arcidiacono[a,c,13], S. Argiro[a,b], M. Arneodo[a,c], N. Bartosik[a], R. Bellan[a,b], C. Biino[a], N. Cartiglia[a], M. Costa[a,b], R. Covarelli[a,b], A. Degano[a,b], N. Demaria[a], L. Finco[a,b], B. Kiani[a,b], C. Mariotti[a], S. Maselli[a], E. Migliore[a,b], V. Monaco[a,b], E. Monteil[a,b], M.M. Obertino[a,b], L. Pacher[a,b], N. Pastrone[a], M. Pelliccioni[a], G.L. Pinna Angioni[a,b], F. Ravera[a,b], A. Romero[a,b], M. Ruspa[a,c], R. Sacchi[a,b], V. Sola[a], A. Solano[a,b], A. Staiano[a], P. Traczyk[a,b]

INFN Sezione di Trieste [a], Università di Trieste [b], Trieste, Italy
S. Belforte[a], V. Candelise[a,b], M. Casarsa[a], F. Cossutti[a], G. Della Ricca[a,b], C. La Licata[a,b], A. Schizzi[a,b], A. Zanetti[a]

Kangwon National University, Chunchon, Korea
S.K. Nam

Kyungpook National University, Daegu, Korea
D.H. Kim, G.N. Kim, M.S. Kim, D.J. Kong, S. Lee, S.W. Lee, Y.D. Oh, A. Sakharov, D.C. Son, Y.C. Yang

Chonbuk National University, Jeonju, Korea
J.A. Brochero Cifuentes, H. Kim, T.J. Kim[31]

Chonnam National University, Institute for Universe and Elementary Particles, Kwangju, Korea
S. Song

Korea University, Seoul, Korea
S. Cho, S. Choi, Y. Go, D. Gyun, B. Hong, Y. Jo, Y. Kim, B. Lee, K. Lee, K.S. Lee, S. Lee, J. Lim, S.K. Park, Y. Roh

Seoul National University, Seoul, Korea
H.D. Yoo

University of Seoul, Seoul, Korea
M. Choi, H. Kim, H. Kim, J.H. Kim, J.S.H. Lee, I.C. Park, G. Ryu, M.S. Ryu

Sungkyunkwan University, Suwon, Korea
Y. Choi, J. Goh, D. Kim, E. Kwon, J. Lee, I. Yu

Vilnius University, Vilnius, Lithuania
V. Dudenas, A. Juodagalvis, J. Vaitkus

National Centre for Particle Physics, Universiti Malaya, Kuala Lumpur, Malaysia
I. Ahmed, Z.A. Ibrahim, J.R. Komaragiri, M.A.B. Md Ali[32], F. Mohamad Idris[33], W.A.T. Wan Abdullah, M.N. Yusli, Z. Zolkapli

Centro de Investigacion y de Estudios Avanzados del IPN, Mexico City, Mexico
E. Casimiro Linares, H. Castilla-Valdez, E. De La Cruz-Burelo, I. Heredia-De La Cruz[34], A. Hernandez-Almada, R. Lopez-Fernandez, J. Mejia Guisao, A. Sanchez-Hernandez

Universidad Iberoamericana, Mexico City, Mexico
S. Carrillo Moreno, F. Vazquez Valencia

Benemerita Universidad Autonoma de Puebla, Puebla, Mexico
I. Pedraza, H.A. Salazar Ibarguen, C. Uribe Estrada

Universidad Autónoma de San Luis Potosí, San Luis Potosí, Mexico
A. Morelos Pineda

University of Auckland, Auckland, New Zealand
D. Krofcheck

University of Canterbury, Christchurch, New Zealand
P.H. Butler

National Centre for Physics, Quaid-I-Azam University, Islamabad, Pakistan
A. Ahmad, M. Ahmad, Q. Hassan, H.R. Hoorani, W.A. Khan, T. Khurshid, M. Shoaib, M. Waqas

National Centre for Nuclear Research, Swierk, Poland
H. Bialkowska, M. Bluj, B. Boimska, T. Frueboes, M. Górski, M. Kazana, K. Nawrocki, K. Romanowska-Rybinska, M. Szleper, P. Zalewski

Institute of Experimental Physics, Faculty of Physics, University of Warsaw, Warsaw, Poland
G. Brona, K. Bunkowski, A. Byszuk[35], K. Doroba, A. Kalinowski, M. Konecki, J. Krolikowski, M. Misiura, M. Olszewski, M. Walczak

Laboratório de Instrumentação e Física Experimental de Partículas, Lisboa, Portugal
P. Bargassa, C. Beirão Da Cruz E Silva, A. Di Francesco, P. Faccioli, P.G. Ferreira Parracho, M. Gallinaro, J. Hollar, N. Leonardo, L. Lloret Iglesias, M.V. Nemallapudi, F. Nguyen, J. Rodrigues Antunes, J. Seixas, O. Toldaiev, D. Vadruccio, J. Varela, P. Vischia

Joint Institute for Nuclear Research, Dubna, Russia
S. Afanasiev, P. Bunin, I. Golutvin, A. Kamenev, V. Karjavin, V. Korenkov, A. Lanev, A. Malakhov, V. Matveev[36,37], V.V. Mitsyn, P. Moisenz, V. Palichik, V. Perelygin, M. Savina, S. Shmatov, N. Skatchkov, V. Smirnov, N. Voytishin, A. Zarubin

Petersburg Nuclear Physics Institute, Gatchina (St. Petersburg), Russia
V. Golovtsov, Y. Ivanov, V. Kim[38], E. Kuznetsova[39], P. Levchenko, V. Murzin, V. Oreshkin, I. Smirnov, V. Sulimov, L. Uvarov, S. Vavilov, A. Vorobyev

Institute for Nuclear Research, Moscow, Russia
Yu. Andreev, A. Dermenev, S. Gninenko, N. Golubev, A. Karneyeu, M. Kirsanov, N. Krasnikov, A. Pashenkov, D. Tlisov, A. Toropin

Institute for Theoretical and Experimental Physics, Moscow, Russia
V. Epshteyn, V. Gavrilov, N. Lychkovskaya, V. Popov, I. Pozdnyakov, G. Safronov, A. Spiridonov, M. Toms, E. Vlasov, A. Zhokin

National Research Nuclear University 'Moscow Engineering Physics Institute' (MEPhI), Moscow, Russia
M. Chadeeva, R. Chistov, M. Danilov, O. Markin, E. Tarkovskii

P.N. Lebedev Physical Institute, Moscow, Russia
V. Andreev, M. Azarkin[37], I. Dremin[37], M. Kirakosyan, A. Leonidov[37], G. Mesyats, S.V. Rusakov

Skobeltsyn Institute of Nuclear Physics, Lomonosov Moscow State University, Moscow, Russia
A. Baskakov, A. Belyaev, E. Boos, V. Bunichev, M. Dubinin[40], L. Dudko, A. Gribushin, V. Klyukhin, O. Kodolova, I. Lokhtin, I. Miagkov, S. Obraztsov, S. Petrushanko, V. Savrin, A. Snigirev

State Research Center of Russian Federation, Institute for High Energy Physics, Protvino, Russia
I. Azhgirey, I. Bayshev, S. Bitioukov, V. Kachanov, A. Kalinin, D. Konstantinov, V. Krychkine, V. Petrov, R. Ryutin, A. Sobol, L. Tourtchanovitch, S. Troshin, N. Tyurin, A. Uzunian, A. Volkov

University of Belgrade, Faculty of Physics and Vinca Institute of Nuclear Sciences, Belgrade, Serbia
P. Adzic[41], P. Cirkovic, D. Devetak, J. Milosevic, V. Rekovic

Centro de Investigaciones Energéticas Medioambientales y Tecnológicas (CIEMAT), Madrid, Spain
J. Alcaraz Maestre, E. Calvo, M. Cerrada, M. Chamizo Llatas, N. Colino, B. De La Cruz, A. Delgado Peris, A. Escalante Del Valle, C. Fernandez Bedoya, J.P. Fernández Ramos, J. Flix, M.C. Fouz, P. Garcia-Abia, O. Gonzalez Lopez, S. Goy Lopez, J.M. Hernandez, M.I. Josa, E. Navarro De Martino, A. Pérez-Calero Yzquierdo, J. Puerta Pelayo, A. Quintario Olmeda, I. Redondo, L. Romero, M.S. Soares

Universidad Autónoma de Madrid, Madrid, Spain
J.F. de Trocóniz, M. Missiroli, D. Moran

Universidad de Oviedo, Oviedo, Spain
J. Cuevas, J. Fernandez Menendez, S. Folgueras, I. Gonzalez Caballero, E. Palencia Cortezon, J.M. Vizan Garcia

Instituto de Física de Cantabria (IFCA), CSIC-Universidad de Cantabria, Santander, Spain
I.J. Cabrillo, A. Calderon, J.R. Castiñeiras De Saa, E. Curras, M. Fernandez, J. Garcia-Ferrero, G. Gomez, A. Lopez Virto, J. Marco, R. Marco, C. Martinez Rivero, F. Matorras, J. Piedra Gomez, T. Rodrigo, A.Y. Rodríguez-Marrero, A. Ruiz-Jimeno, L. Scodellaro, N. Trevisani, I. Vila, R. Vilar Cortabitarte

CERN, European Organization for Nuclear Research, Geneva, Switzerland
D. Abbaneo, E. Auffray, G. Auzinger, M. Bachtis, P. Baillon, A.H. Ball, D. Barney, A. Benaglia, L. Benhabib, G.M. Berruti, P. Bloch, A. Bocci, A. Bonato, C. Botta, H. Breuker, T. Camporesi, R. Castello, M. Cepeda, G. Cerminara, M. D'Alfonso, D. d'Enterria, A. Dabrowski, V. Daponte, A. David, M. De Gruttola, F. De Guio, A. De Roeck, E. Di Marco[42], M. Dobson, M. Dordevic, B. Dorney, T. du Pree, D. Duggan, M. Dünser, N. Dupont, A. Elliott-Peisert, S. Fartoukh, G. Franzoni, J. Fulcher, W. Funk, D. Gigi, K. Gill, M. Girone, F. Glege, R. Guida, S. Gundacker, M. Guthoff, J. Hammer, P. Harris, J. Hegeman, V. Innocente, P. Janot, H. Kirschenmann, V. Knünz, M.J. Kortelainen, K. Kousouris, P. Lecoq, C. Lourenço, M.T. Lucchini, N. Magini, L. Malgeri, M. Mannelli, A. Martelli, L. Masetti, F. Meijers, S. Mersi, E. Meschi, F. Moortgat, S. Morovic, M. Mulders, H. Neugebauer, S. Orfanelli[43], L. Orsini, L. Pape, E. Perez, M. Peruzzi, A. Petrilli, G. Petrucciani, A. Pfeiffer, M. Pierini, D. Piparo, A. Racz, T. Reis, G. Rolandi[44], M. Rovere, M. Ruan, H. Sakulin, J.B. Sauvan, C. Schäfer, C. Schwick, M. Seidel, A. Sharma, P. Silva, M. Simon, P. Sphicas[45], J. Steggemann, M. Stoye, Y. Takahashi, D. Treille, A. Triossi, A. Tsirou, V. Veckalns[46], G.I. Veres[20], N. Wardle, H.K. Wöhri, A. Zagozdzinska[35], W.D. Zeuner

Paul Scherrer Institut, Villigen, Switzerland
W. Bertl, K. Deiters, W. Erdmann, R. Horisberger, Q. Ingram, H.C. Kaestli, D. Kotlinski, U. Langenegger, T. Rohe

Institute for Particle Physics, ETH Zurich, Zurich, Switzerland
F. Bachmair, L. Bäni, L. Bianchini, B. Casal, G. Dissertori, M. Dittmar, M. Donegà, P. Eller, C. Grab, C. Heidegger, D. Hits, J. Hoss, G. Kasieczka, P. Lecomte†, W. Lustermann, B. Mangano, M. Marionneau, P. Martinez Ruiz del Arbol, M. Masciovecchio, M.T. Meinhard, D. Meister, F. Micheli, P. Musella, F. Nessi-Tedaldi, F. Pandolfi, J. Pata, F. Pauss, G. Perrin, L. Perrozzi, M. Quittnat, M. Rossini, M. Schönenberger, A. Starodumov[47], M. Takahashi, V.R. Tavolaro, K. Theofilatos, R. Wallny

Universität Zürich, Zurich, Switzerland
T.K. Aarrestad, C. Amsler[48], L. Caminada, M.F. Canelli, V. Chiochia, A. De Cosa, C. Galloni, A. Hinzmann, T. Hreus, B. Kilminster, C. Lange, J. Ngadiuba, D. Pinna, G. Rauco, P. Robmann, D. Salerno, Y. Yang

National Central University, Chung-Li, Taiwan
K.H. Chen, T.H. Doan, Sh. Jain, R. Khurana, M. Konyushikhin, C.M. Kuo, W. Lin, Y.J. Lu, A. Pozdnyakov, S.S. Yu

National Taiwan University (NTU), Taipei, Taiwan
Arun Kumar, P. Chang, Y.H. Chang, Y.W. Chang, Y. Chao, K.F. Chen, P.H. Chen, C. Dietz, F. Fiori, W.-S. Hou, Y. Hsiung, Y.F. Liu, R.-S. Lu, M. Miñano Moya, J.f. Tsai, Y.M. Tzeng

Chulalongkorn University, Faculty of Science, Department of Physics, Bangkok, Thailand
B. Asavapibhop, K. Kovitanggoon, G. Singh, N. Srimanobhas, N. Suwonjandee

Cukurova University, Adana, Turkey
A. Adiguzel, S. Cerci[49], S. Damarseckin, Z.S. Demiroglu, C. Dozen, I. Dumanoglu, S. Girgis, G. Gokbulut, Y. Guler, E. Gurpinar, I. Hos, E.E. Kangal[50], A. Kayis Topaksu, G. Onengut[51], K. Ozdemir[52], S. Ozturk[53], B. Tali[49], H. Topakli[53], C. Zorbilmez

Middle East Technical University, Physics Department, Ankara, Turkey
B. Bilin, S. Bilmis, B. Isildak[54], G. Karapinar[55], M. Yalvac, M. Zeyrek

Bogazici University, Istanbul, Turkey
E. Gülmez, M. Kaya[56], O. Kaya[57], E.A. Yetkin[58], T. Yetkin[59]

Istanbul Technical University, Istanbul, Turkey
A. Cakir, K. Cankocak, S. Sen[60], F.I. Vardarlı

Institute for Scintillation Materials of National Academy of Science of Ukraine, Kharkov, Ukraine
B. Grynyov

National Scientific Center, Kharkov Institute of Physics and Technology, Kharkov, Ukraine
L. Levchuk, P. Sorokin

University of Bristol, Bristol, United Kingdom
R. Aggleton, F. Ball, L. Beck, J.J. Brooke, D. Burns, E. Clement, D. Cussans, H. Flacher, J. Goldstein, M. Grimes, G.P. Heath, H.F. Heath, J. Jacob, L. Kreczko, C. Lucas, Z. Meng, D.M. Newbold[61], S. Paramesvaran, A. Poll, T. Sakuma, S. Seif El Nasr-storey, S. Senkin, D. Smith, V.J. Smith

Rutherford Appleton Laboratory, Didcot, United Kingdom
K.W. Bell, A. Belyaev[62], C. Brew, R.M. Brown, L. Calligaris, D. Cieri, D.J.A. Cockerill, J.A. Coughlan, K. Harder, S. Harper, E. Olaiya, D. Petyt, C.H. Shepherd-Themistocleous, A. Thea, I.R. Tomalin, T. Williams, S.D. Worm

Imperial College, London, United Kingdom
M. Baber, R. Bainbridge, O. Buchmuller, A. Bundock, D. Burton, S. Casasso, M. Citron, D. Colling, L. Corpe, P. Dauncey, G. Davies, A. De Wit, M. Della Negra, P. Dunne, A. Elwood, D. Futyan, Y. Haddad, G. Hall, G. Iles, R. Lane, R. Lucas[61], L. Lyons, A.-M. Magnan, S. Malik, L. Mastrolorenzo, J. Nash, A. Nikitenko[47], J. Pela, B. Penning, M. Pesaresi, D.M. Raymond, A. Richards, A. Rose, C. Seez, A. Tapper, K. Uchida, M. Vazquez Acosta[63], T. Virdee[13], S.C. Zenz

Brunel University, Uxbridge, United Kingdom
J.E. Cole, P.R. Hobson, A. Khan, P. Kyberd, D. Leslie, I.D. Reid, P. Symonds, L. Teodorescu, M. Turner

Baylor University, Waco, USA
A. Borzou, K. Call, J. Dittmann, K. Hatakeyama, H. Liu, N. Pastika

The University of Alabama, Tuscaloosa, USA
O. Charaf, S.I. Cooper, C. Henderson, P. Rumerio

Boston University, Boston, USA
D. Arcaro, A. Avetisyan, T. Bose, D. Gastler, D. Rankin, C. Richardson, J. Rohlf, L. Sulak, D. Zou

Brown University, Providence, USA
J. Alimena, G. Benelli, E. Berry, D. Cutts, A. Ferapontov, A. Garabedian, J. Hakala, U. Heintz, O. Jesus, E. Laird, G. Landsberg, Z. Mao, M. Narain, S. Piperov, S. Sagir, R. Syarif

University of California, Davis, Davis, USA
R. Breedon, G. Breto, M. Calderon De La Barca Sanchez, S. Chauhan, M. Chertok, J. Conway, R. Conway, P.T. Cox, R. Erbacher, C. Flores, G. Funk, M. Gardner, W. Ko, R. Lander, C. Mclean, M. Mulhearn, D. Pellett, J. Pilot, F. Ricci-Tam, S. Shalhout, J. Smith, M. Squires, D. Stolp, M. Tripathi, S. Wilbur, R. Yohay

University of California, Los Angeles, USA
R. Cousins, P. Everaerts, A. Florent, J. Hauser, M. Ignatenko, D. Saltzberg, E. Takasugi, V. Valuev, M. Weber

University of California, Riverside, Riverside, USA
K. Burt, R. Clare, J. Ellison, J.W. Gary, G. Hanson, J. Heilman, P. Jandir, E. Kennedy, F. Lacroix, O.R. Long, M. Malberti, M. Olmedo Negrete, M.I. Paneva, A. Shrinivas, H. Wei, S. Wimpenny, B. R. Yates

University of California, San Diego, La Jolla, USA
J.G. Branson, G.B. Cerati, S. Cittolin, R.T. D'Agnolo, M. Derdzinski, R. Gerosa, A. Holzner, R. Kelley, D. Klein, J. Letts, I. Macneill, D. Olivito, S. Padhi, M. Pieri, M. Sani, V. Sharma, S. Simon, M. Tadel, A. Vartak, S. Wasserbaech[64], C. Welke, J. Wood, F. Würthwein, A. Yagil, G. Zevi Della Porta

University of California, Santa Barbara, Santa Barbara, USA
J. Bradmiller-Feld, C. Campagnari, A. Dishaw, V. Dutta, K. Flowers, M. Franco Sevilla, P. Geffert, C. George, F. Golf, L. Gouskos, J. Gran, J. Incandela, N. Mccoll, S.D. Mullin, J. Richman, D. Stuart, I. Suarez, C. West, J. Yoo

California Institute of Technology, Pasadena, USA
D. Anderson, A. Apresyan, J. Bendavid, A. Bornheim, J. Bunn, Y. Chen, J. Duarte, A. Mott, H.B. Newman, C. Pena, M. Spiropulu, J.R. Vlimant, S. Xie, R.Y. Zhu

Carnegie Mellon University, Pittsburgh, USA
M.B. Andrews, V. Azzolini, A. Calamba, B. Carlson, T. Ferguson, M. Paulini, J. Russ, M. Sun, H. Vogel, I. Vorobiev

University of Colorado Boulder, Boulder, USA
J.P. Cumalat, W.T. Ford, F. Jensen, A. Johnson, M. Krohn, T. Mulholland, K. Stenson, S.R. Wagner

Cornell University, Ithaca, USA
J. Alexander, A. Chatterjee, J. Chaves, J. Chu, S. Dittmer, N. Eggert, N. Mirman, G. Nicolas Kaufman, J.R. Patterson, A. Rinkevicius, A. Ryd, L. Skinnari, L. Soffi, W. Sun, S.M. Tan, W.D. Teo, J. Thom, J. Thompson, J. Tucker, Y. Weng, P. Wittich

Fermi National Accelerator Laboratory, Batavia, USA
S. Abdullin, M. Albrow, G. Apollinari, S. Banerjee, L.A.T. Bauerdick, A. Beretvas, J. Berryhill, P.C. Bhat, G. Bolla, K. Burkett, J.N. Butler, H.W.K. Cheung, F. Chlebana, S. Cihangir, M. Cremonesi, V.D. Elvira, I. Fisk, J. Freeman, E. Gottschalk, L. Gray, D. Green, S. Grünendahl, O. Gutsche, D. Hare, R.M. Harris, S. Hasegawa, J. Hirschauer, Z. Hu, B. Jayatilaka, S. Jindariani, M. Johnson, U. Joshi, B. Klima, B. Kreis, S. Lammel, J. Lewis, J. Linacre, D. Lincoln, R. Lipton, T. Liu, R. Lopes De Sá, J. Lykken, K. Maeshima, J.M. Marraffino, S. Maruyama, D. Mason,

P. McBride, P. Merkel, S. Mrenna, S. Nahn, C. Newman-Holmes†, V. O'Dell, K. Pedro, O. Prokofyev, G. Rakness, E. Sexton-Kennedy, A. Soha, W.J. Spalding, L. Spiegel, S. Stoynev, N. Strobbe, L. Taylor, S. Tkaczyk, N.V. Tran, L. Uplegger, E.W. Vaandering, C. Vernieri, M. Verzocchi, R. Vidal, M. Wang, H.A. Weber, A. Whitbeck

University of Florida, Gainesville, USA
D. Acosta, P. Avery, P. Bortignon, D. Bourilkov, A. Brinkerhoff, A. Carnes, M. Carver, D. Curry, S. Das, R.D. Field, I.K. Furic, J. Konigsberg, A. Korytov, K. Kotov, P. Ma, K. Matchev, H. Mei, P. Milenovic[65], G. Mitselmakher, D. Rank, R. Rossin, L. Shchutska, D. Sperka, N. Terentyev, L. Thomas, J. Wang, S. Wang, J. Yelton

Florida International University, Miami, USA
S. Linn, P. Markowitz, G. Martinez, J.L. Rodriguez

Florida State University, Tallahassee, USA
A. Ackert, J.R. Adams, T. Adams, A. Askew, S. Bein, J. Bochenek, B. Diamond, J. Haas, S. Hagopian, V. Hagopian, K.F. Johnson, A. Khatiwada, H. Prosper, A. Santra, M. Weinberg

Florida Institute of Technology, Melbourne, USA
M.M. Baarmand, V. Bhopatkar, S. Colafranceschi[66], M. Hohlmann, H. Kalakhety, D. Noonan, T. Roy, F. Yumiceva

University of Illinois at Chicago (UIC), Chicago, USA
M.R. Adams, L. Apanasevich, D. Berry, R.R. Betts, I. Bucinskaite, R. Cavanaugh, O. Evdokimov, L. Gauthier, C.E. Gerber, D.J. Hofman, P. Kurt, C. O'Brien, I.D. Sandoval Gonzalez, P. Turner, N. Varelas, Z. Wu, M. Zakaria, J. Zhang

The University of Iowa, Iowa City, USA
B. Bilki[67], W. Clarida, K. Dilsiz, S. Durgut, R.P. Gandrajula, M. Haytmyradov, V. Khristenko, J.-P. Merlo, H. Mermerkaya[68], A. Mestvirishvili, A. Moeller, J. Nachtman, H. Ogul, Y. Onel, F. Ozok[69], A. Penzo, C. Snyder, E. Tiras, J. Wetzel, K. Yi

Johns Hopkins University, Baltimore, USA
I. Anderson, B. Blumenfeld, A. Cocoros, N. Eminizer, D. Fehling, L. Feng, A.V. Gritsan, P. Maksimovic, M. Osherson, J. Roskes, U. Sarica, M. Swartz, M. Xiao, Y. Xin, C. You

The University of Kansas, Lawrence, USA
P. Baringer, A. Bean, C. Bruner, J. Castle, R.P. Kenny III, A. Kropivnitskaya, D. Majumder, M. Malek, W. Mcbrayer, M. Murray, S. Sanders, R. Stringer, Q. Wang

Kansas State University, Manhattan, USA
A. Ivanov, K. Kaadze, S. Khalil, M. Makouski, Y. Maravin, A. Mohammadi, L.K. Saini, N. Skhirtladze, S. Toda

Lawrence Livermore National Laboratory, Livermore, USA
D. Lange, F. Rebassoo, D. Wright

University of Maryland, College Park, USA
C. Anelli, A. Baden, O. Baron, A. Belloni, B. Calvert, S.C. Eno, C. Ferraioli, J.A. Gomez, N.J. Hadley, S. Jabeen, R.G. Kellogg, T. Kolberg, J. Kunkle, Y. Lu, A.C. Mignerey, Y.H. Shin, A. Skuja, M.B. Tonjes, S.C. Tonwar

Massachusetts Institute of Technology, Cambridge, USA
A. Apyan, R. Barbieri, A. Baty, R. Bi, K. Bierwagen, S. Brandt, W. Busza, I.A. Cali, Z. Demiragli, L. Di Matteo, G. Gomez Ceballos, M. Goncharov, D. Gulhan, D. Hsu, Y. Iiyama, G.M. Innocenti,

M. Klute, D. Kovalskyi, K. Krajczar, Y.S. Lai, Y.-J. Lee, A. Levin, P.D. Luckey, A.C. Marini, C. Mcginn, C. Mironov, S. Narayanan, X. Niu, C. Paus, C. Roland, G. Roland, J. Salfeld-Nebgen, G.S.F. Stephans, K. Sumorok, K. Tatar, M. Varma, D. Velicanu, J. Veverka, J. Wang, T.W. Wang, B. Wyslouch, M. Yang, V. Zhukova

University of Minnesota, Minneapolis, USA
A.C. Benvenuti, B. Dahmes, A. Evans, A. Finkel, A. Gude, P. Hansen, S. Kalafut, S.C. Kao, K. Klapoetke, Y. Kubota, Z. Lesko, J. Mans, S. Nourbakhsh, N. Ruckstuhl, R. Rusack, N. Tambe, J. Turkewitz

University of Mississippi, Oxford, USA
J.G. Acosta, S. Oliveros

University of Nebraska-Lincoln, Lincoln, USA
E. Avdeeva, R. Bartek, K. Bloom, S. Bose, D.R. Claes, A. Dominguez, C. Fangmeier, R. Gonzalez Suarez, R. Kamalieddin, D. Knowlton, I. Kravchenko, F. Meier, J. Monroy, F. Ratnikov, J.E. Siado, G.R. Snow, B. Stieger

State University of New York at Buffalo, Buffalo, USA
M. Alyari, J. Dolen, J. George, A. Godshalk, C. Harrington, I. Iashvili, J. Kaisen, A. Kharchilava, A. Kumar, A. Parker, S. Rappoccio, B. Roozbahani

Northeastern University, Boston, USA
G. Alverson, E. Barberis, D. Baumgartel, M. Chasco, A. Hortiangtham, A. Massironi, D.M. Morse, D. Nash, T. Orimoto, R. Teixeira De Lima, D. Trocino, R.-J. Wang, D. Wood, J. Zhang

Northwestern University, Evanston, USA
S. Bhattacharya, K.A. Hahn, A. Kubik, J.F. Low, N. Mucia, N. Odell, B. Pollack, M.H. Schmitt, K. Sung, M. Trovato, M. Velasco

University of Notre Dame, Notre Dame, USA
N. Dev, M. Hildreth, C. Jessop, D.J. Karmgard, N. Kellams, K. Lannon, N. Marinelli, F. Meng, C. Mueller, Y. Musienko[36], M. Planer, A. Reinsvold, R. Ruchti, N. Rupprecht, G. Smith, S. Taroni, N. Valls, M. Wayne, M. Wolf, A. Woodard

The Ohio State University, Columbus, USA
L. Antonelli, J. Brinson, B. Bylsma, L.S. Durkin, S. Flowers, A. Hart, C. Hill, R. Hughes, W. Ji, B. Liu, W. Luo, D. Puigh, M. Rodenburg, B.L. Winer, H.W. Wulsin

Princeton University, Princeton, USA
O. Driga, P. Elmer, J. Hardenbrook, P. Hebda, S.A. Koay, P. Lujan, D. Marlow, T. Medvedeva, M. Mooney, J. Olsen, C. Palmer, P. Piroué, D. Stickland, C. Tully, A. Zuranski

University of Puerto Rico, Mayaguez, USA
S. Malik

Purdue University, West Lafayette, USA
A. Barker, V.E. Barnes, D. Benedetti, L. Gutay, M.K. Jha, M. Jones, A.W. Jung, K. Jung, D.H. Miller, N. Neumeister, B.C. Radburn-Smith, X. Shi, J. Sun, A. Svyatkovskiy, F. Wang, W. Xie, L. Xu

Purdue University Calumet, Hammond, USA
N. Parashar, J. Stupak

Rice University, Houston, USA
A. Adair, B. Akgun, Z. Chen, K.M. Ecklund, F.J.M. Geurts, M. Guilbaud, W. Li, B. Michlin, M. Northup, B.P. Padley, R. Redjimi, J. Roberts, J. Rorie, Z. Tu, J. Zabel

University of Rochester, Rochester, USA
B. Betchart, A. Bodek, P. de Barbaro, R. Demina, Y.t. Duh, Y. Eshaq, T. Ferbel, M. Galanti, A. Garcia-Bellido, J. Han, O. Hindrichs, A. Khukhunaishvili, K.H. Lo, P. Tan, M. Verzetti

Rutgers, The State University of New Jersey, Piscataway, USA
J.P. Chou, E. Contreras-Campana, Y. Gershtein, T.A. Gómez Espinosa, E. Halkiadakis, M. Heindl, D. Hidas, E. Hughes, S. Kaplan, R. Kunnawalkam Elayavalli, S. Kyriacou, A. Lath, K. Nash, H. Saka, S. Salur, S. Schnetzer, D. Sheffield, S. Somalwar, R. Stone, S. Thomas, P. Thomassen, M. Walker

University of Tennessee, Knoxville, USA
M. Foerster, J. Heideman, G. Riley, K. Rose, S. Spanier, K. Thapa

Texas A&M University, College Station, USA
O. Bouhali[70], A. Castaneda Hernandez[70], A. Celik, M. Dalchenko, M. De Mattia, A. Delgado, S. Dildick, R. Eusebi, J. Gilmore, T. Huang, T. Kamon[71], V. Krutelyov, R. Mueller, I. Osipenkov, Y. Pakhotin, R. Patel, A. Perloff, L. Perniè, D. Rathjens, A. Rose, A. Safonov, A. Tatarinov, K.A. Ulmer

Texas Tech University, Lubbock, USA
N. Akchurin, C. Cowden, J. Damgov, C. Dragoiu, P.R. Dudero, J. Faulkner, S. Kunori, K. Lamichhane, S.W. Lee, T. Libeiro, S. Undleeb, I. Volobouev, Z. Wang

Vanderbilt University, Nashville, USA
E. Appelt, A.G. Delannoy, S. Greene, A. Gurrola, R. Janjam, W. Johns, C. Maguire, Y. Mao, A. Melo, H. Ni, P. Sheldon, S. Tuo, J. Velkovska, Q. Xu

University of Virginia, Charlottesville, USA
M.W. Arenton, P. Barria, B. Cox, B. Francis, J. Goodell, R. Hirosky, A. Ledovskoy, H. Li, C. Neu, T. Sinthuprasith, X. Sun, Y. Wang, E. Wolfe, F. Xia

Wayne State University, Detroit, USA
C. Clarke, R. Harr, P.E. Karchin, C. Kottachchi Kankanamge Don, P. Lamichhane, J. Sturdy

University of Wisconsin - Madison, Madison, WI, USA
D.A. Belknap, D. Carlsmith, S. Dasu, L. Dodd, S. Duric, B. Gomber, M. Grothe, M. Herndon, A. Hervé, P. Klabbers, A. Lanaro, A. Levine, K. Long, R. Loveless, A. Mohapatra, I. Ojalvo, T. Perry, G.A. Pierro, G. Polese, T. Ruggles, T. Sarangi, A. Savin, A. Sharma, N. Smith, W.H. Smith, D. Taylor, P. Verwilligen, N. Woods

†: Deceased
1: Also at Vienna University of Technology, Vienna, Austria
2: Also at State Key Laboratory of Nuclear Physics and Technology, Peking University, Beijing, China
3: Also at Institut Pluridisciplinaire Hubert Curien, Université de Strasbourg, Université de Haute Alsace Mulhouse, CNRS/IN2P3, Strasbourg, France
4: Also at Universidade Estadual de Campinas, Campinas, Brazil
5: Also at Centre National de la Recherche Scientifique (CNRS) - IN2P3, Paris, France
6: Also at Université Libre de Bruxelles, Bruxelles, Belgium
7: Also at Laboratoire Leprince-Ringuet, Ecole Polytechnique, IN2P3-CNRS, Palaiseau, France

8: Also at Joint Institute for Nuclear Research, Dubna, Russia
9: Now at British University in Egypt, Cairo, Egypt
10: Also at Zewail City of Science and Technology, Zewail, Egypt
11: Now at Ain Shams University, Cairo, Egypt
12: Also at Université de Haute Alsace, Mulhouse, France
13: Also at CERN, European Organization for Nuclear Research, Geneva, Switzerland
14: Also at Skobeltsyn Institute of Nuclear Physics, Lomonosov Moscow State University, Moscow, Russia
15: Also at Tbilisi State University, Tbilisi, Georgia
16: Also at RWTH Aachen University, III. Physikalisches Institut A, Aachen, Germany
17: Also at University of Hamburg, Hamburg, Germany
18: Also at Brandenburg University of Technology, Cottbus, Germany
19: Also at Institute of Nuclear Research ATOMKI, Debrecen, Hungary
20: Also at MTA-ELTE Lendület CMS Particle and Nuclear Physics Group, Eötvös Loránd University, Budapest, Hungary
21: Also at University of Debrecen, Debrecen, Hungary
22: Also at Indian Institute of Science Education and Research, Bhopal, India
23: Also at University of Visva-Bharati, Santiniketan, India
24: Now at King Abdulaziz University, Jeddah, Saudi Arabia
25: Also at University of Ruhuna, Matara, Sri Lanka
26: Also at Isfahan University of Technology, Isfahan, Iran
27: Also at University of Tehran, Department of Engineering Science, Tehran, Iran
28: Also at Plasma Physics Research Center, Science and Research Branch, Islamic Azad University, Tehran, Iran
29: Also at Università degli Studi di Siena, Siena, Italy
30: Also at Purdue University, West Lafayette, USA
31: Now at Hanyang University, Seoul, Korea
32: Also at International Islamic University of Malaysia, Kuala Lumpur, Malaysia
33: Also at Malaysian Nuclear Agency, MOSTI, Kajang, Malaysia
34: Also at Consejo Nacional de Ciencia y Tecnología, Mexico city, Mexico
35: Also at Warsaw University of Technology, Institute of Electronic Systems, Warsaw, Poland
36: Also at Institute for Nuclear Research, Moscow, Russia
37: Now at National Research Nuclear University 'Moscow Engineering Physics Institute' (MEPhI), Moscow, Russia
38: Also at St. Petersburg State Polytechnical University, St. Petersburg, Russia
39: Also at University of Florida, Gainesville, USA
40: Also at California Institute of Technology, Pasadena, USA
41: Also at Faculty of Physics, University of Belgrade, Belgrade, Serbia
42: Also at INFN Sezione di Roma; Università di Roma, Roma, Italy
43: Also at National Technical University of Athens, Athens, Greece
44: Also at Scuola Normale e Sezione dell'INFN, Pisa, Italy
45: Also at National and Kapodistrian University of Athens, Athens, Greece
46: Also at Riga Technical University, Riga, Latvia
47: Also at Institute for Theoretical and Experimental Physics, Moscow, Russia
48: Also at Albert Einstein Center for Fundamental Physics, Bern, Switzerland
49: Also at Adiyaman University, Adiyaman, Turkey
50: Also at Mersin University, Mersin, Turkey
51: Also at Cag University, Mersin, Turkey
52: Also at Piri Reis University, Istanbul, Turkey

53: Also at Gaziosmanpasa University, Tokat, Turkey
54: Also at Ozyegin University, Istanbul, Turkey
55: Also at Izmir Institute of Technology, Izmir, Turkey
56: Also at Marmara University, Istanbul, Turkey
57: Also at Kafkas University, Kars, Turkey
58: Also at Istanbul Bilgi University, Istanbul, Turkey
59: Also at Yildiz Technical University, Istanbul, Turkey
60: Also at Hacettepe University, Ankara, Turkey
61: Also at Rutherford Appleton Laboratory, Didcot, United Kingdom
62: Also at School of Physics and Astronomy, University of Southampton, Southampton, United Kingdom
63: Also at Instituto de Astrofísica de Canarias, La Laguna, Spain
64: Also at Utah Valley University, Orem, USA
65: Also at University of Belgrade, Faculty of Physics and Vinca Institute of Nuclear Sciences, Belgrade, Serbia
66: Also at Facoltà Ingegneria, Università di Roma, Roma, Italy
67: Also at Argonne National Laboratory, Argonne, USA
68: Also at Erzincan University, Erzincan, Turkey
69: Also at Mimar Sinan University, Istanbul, Istanbul, Turkey
70: Also at Texas A&M University at Qatar, Doha, Qatar
71: Also at Kyungpook National University, Daegu, Korea